THE JOURNAL OF BIOLOGICAL CHEMISTRY VOL. 286, NO. 49, pp. 42162–42179, December 9, 2011

Carbohydrate Metabolism Is Perturbed in Peroxisome-deficient Hepatocytes Due to Mitochondrial Dysfunction, AMP-activated Protein Kinase (AMPK) Activation, and Peroxisome Proliferator-activated Receptor γ Coactivator 1α (PGC-1α) Suppression*[S]

Received for publication, September 12, 2011, and in revised form, October 5, 2011 Published, JBC Papers in Press, October 14, 2011, DOI 10.1074/jbc.M111.299727

Annelies Peeters[‡], Peter Fraisl[¶‖], Sjoerd van den Berg[‖], Emiel Ver Loren van Themaat[**], Antoine Van Kampen[**], Mark H. Rider[‡‡], Hiroshi Takemori[§§], Ko Willems van Dijk[‖], Paul P. Van Veldhoven[¶¶], Peter Carmeliet[§¶], and Myriam Baes[‡1]

From the [‡]Laboratory of Cell Metabolism, Department of Pharmaceutical Sciences, [§]Laboratory of Angiogenesis and Neurovascular Link, Vesalius Research Center, and [¶¶]Laboratory of Lipid Biochemistry and Protein Interactions, Department of Molecular Cell Biology, University of Leuven, B-3000 Leuven, Belgium, the [¶]Laboratory of Angiogenesis and Neurovascular Link, Vesalius Research Center, Flanders Institute of Biotechnology, B-3000 Leuven, Belgium, the [‖]Department of Human Genetics, Leiden University Medical Center, NL-2333 ZA Leiden, The Netherlands, the [**]Laboratory of Bioinformatics, Academic Medical Center, NL-1105 AZ Amsterdam, The Netherlands, the [‡‡]Université Catholique de Louvain and de Duve Institute, B-1200 Brussels, Belgium, and the [§§]Laboratory of Cell Signaling and Metabolism,National Institute of Biomedical Innovation, Osaka 567-0085, Japan

Background: It is not known whether peroxisomes influence hepatic carbohydrate metabolism.
Results: Carbohydrate metabolism is perturbed in peroxisome-deficient mouse liver through mitochondrial deficits, AMPK, and PGC-1α.
Conclusion: Dysfunctional peroxisome metabolism disrupts carbohydrate homeostasis by indirect mechanisms.
Significance: The impact of peroxisome deficiency on liver metabolism is broader than expected.

Hepatic peroxisomes are essential for lipid conversions that include the formation of mature conjugated bile acids, the degradation of branched chain fatty acids, and the synthesis of docosahexaenoic acid. Through unresolved mechanisms, deletion of functional peroxisomes from mouse hepatocytes (*L-Pex5*$^{-/-}$ mice) causes severe structural and functional abnormalities at the inner mitochondrial membrane. We now demonstrate that the peroxisomal and mitochondrial anomalies trigger energy deficits, as shown by increased AMP/ATP and decreased NAD^+/NADH ratios. This causes suppression of gluconeogenesis and glycogen synthesis and up-regulation of glycolysis. As a consequence, *L-Pex5*$^{-/-}$ mice combust more carbohydrates resulting in lower body weights despite increased food intake. The perturbation of carbohydrate metabolism does not require a long term adaptation to the absence of functional peroxisomes as similar metabolic changes were also rapidly induced by acute elimination of *Pex5* via adenoviral administration of Cre. Despite its marked activation, peroxisome proliferator-activated receptor α (PPARα) was not causally involved in these metabolic perturbations, because all abnormalities still manifested when peroxisomes were eliminated in a peroxisome proliferator-activated receptor α null background. Instead, AMP-activated kinase activation was responsible for the down-regulation of glycogen synthesis and induction of glycolysis. Remarkably, PGC-1α was suppressed despite AMP-activated kinase activation, a paradigm not previously reported, and they jointly contributed to impaired gluconeogenesis. In conclusion, lack of functional peroxisomes from hepatocytes results in marked disturbances of carbohydrate homeostasis, which are consistent with adaptations to an energy deficit. Because this is primarily due to impaired mitochondrial ATP production, these *L-Pex5*-deficient livers can also be considered as a model for secondary mitochondrial hepatopathies.

Peroxisomes are particularly abundant in hepatocytes where they are responsible for metabolic conversions such as catabolism of branched chain fatty acids and synthesis of polyunsaturated fatty acids and of mature conjugated bile acids (1). Besides this important involvement in lipid metabolism, hepatic peroxisomes are also necessary for the oxidation of urate in certain mammals. As in other tissues, hepatic peroxisomes contain oxidases generating H_2O_2 and superoxide anions, which can be decomposed within the organelle by catalase, glutathione peroxidase, and superoxide dismutases (2).

* This work was funded by Fonds Wetenschappelijk Onderzoek Vlaanderen Grant G.0760.09, Geconcerteerde Onderzoeksacties Grant 2004/08, OT Grant 08/40, European Union Grant LSHG-CT-2004-512018, FP6, the Center of Medical Systems Biology, and the Netherlands Consortium for Systems Biology (established by The Netherlands Genomics Initiative/Netherlands Organization for Scientific Research).
[S] The on-line version of this article (available at http://www.jbc.org) contains supplemental Table 1.
[1] To whom correspondence should be addressed: Laboratory of Cell Metabolism, Faculty of Pharmaceutical Sciences, Campus Gasthuisberg O/N2, Herestraat 49, Box 823, B-3000 Leuven, Belgium. Tel.: 32-16-330853; Fax: 32-16-330856; E-mail: myriam.baes@pharm.kuleuven.be.

In peroxisome biogenesis disorders, such as the cerebrohepatorenal syndrome of Zellweger, functional peroxisomes are absent (3). Because of peroxisome deficiency from hepatocytes, the liver of these patients is already abnormal late in gestation, but hepatic pathology develops actively in the first few weeks of life and usually progresses rapidly. Liver pathology includes hepatomegaly and hepatitis that often rapidly evolves to liver fibrosis and cirrhosis (4). Furthermore, steatosis and canalicular and cytoplasmic cholestasis develop with normal, deficient, or hyperplastic intrahepatic bile ducts. Another striking observation was the altered structure of mitochondria at the level of the inner membrane (5–10). However, the precise consequences of these mitochondrial abnormalities remain largely unexplored.

To better define the role of peroxisomal metabolism in hepatocytes, we recently generated a mouse model with hepatocyte-restricted elimination of functional peroxisomes (*L-Pex5* knock-out mice) (11). These hepatocytes contained mitochondria with severely distorted inner membranes and loss of the mitochondrial membrane potential, strongly reduced activity of complex I, and more moderate impairment of complex III and V. Several PPARα[2] target genes were induced, indicative of the accumulation of PPARα ligands in peroxisome-deficient hepatocytes. Furthermore, the mice displayed microvesicular steatosis and fibrosis and after 12 months hepatocarcinogenesis (11).

During the course of our studies on *L-Pex5* knock-out mice, we found initial evidence of disturbed carbohydrate metabolism, including enhanced glycolysis, but we did not characterize these glucose metabolism abnormalities in detail, and neither did we unravel the underlying mechanisms (11). Therefore, an in-depth analysis of glucose homeostasis was performed revealing impaired gluconeogenesis, glycogen synthesis, and insulin signaling in peroxisome-deficient hepatocytes. Gene expression and activity of key regulators of carbohydrate metabolism were severely disturbed. In particular, the activated AMPK and suppressed PGC-1α were identified to be important regulating factors.

EXPERIMENTAL PROCEDURES

Mouse Breeding

L-Pex5$^{-/-}$ mice were generated by breeding *Pex5*$^{FL/FL}$ mice (12) with *Albumin-Cre* mice (13) as described previously (11). Siblings not expressing CRE recombinase were used as control mice. For all experiments, male animals were used aged between 10 and 20 weeks. Mice were bred in the conventional animal housing facility of the University of Leuven. Animals were maintained on a 12-h light/12-h dark schedule and were fed a standard rodent food chow and water *ad libitum*. *Pex5*$^{FL/FL}$ mice were also brought into a *Ppar*$\alpha^{-/-}$ background (provided by Prof. F. Gonzalez (14)). For certain experiments, *Pex5*$^{FL/FL}$*Ppar*$\alpha^{-/-}$ and *Pex5*$^{FL/FL}$*Ppar*$\alpha^{+/+}$ mice were intravenously injected with $3{\cdot}10^9$ pfu adenovirus expressing CRE recombinase or control adenovirus. All animal experiments were approved by the Institutional Animal Ethical Committee of the University of Leuven.

In Vivo Experiments

Indirect Calorimetry—Indirect calorimetry measurements were performed as reported previously (15). In short, seven mice per group were subjected to individual indirect calorimetry measurements for a period of 5 consecutive days (Comprehensive Laboratory Animal Monitoring System, Columbus Instruments, Columbus, OH). A period of 24 h was included at the start of the experiment to allow acclimatization of the animals to the cages. Food and water were available *ad libitum* during the whole experiment, and intake was analyzed every 10 s. Voluntary physical activity was measured real time as infrared beam breaks in the *X* and *Z* direction. Oxygen consumption (VO_2) and carbon dioxide production rate (VCO_2) measurements were performed at intervals of ~5 min throughout the whole period. Respiratory exchange rate as a measure for metabolic substrate choice was calculated as the ratio between VCO_2 and VO_2. Carbohydrate and fat oxidation rates were calculated according to Peronnet and Massicotte (16). Total energy expenditure was calculated as the sum of carbohydrate and fat oxidation. All measurements were corrected for fat-free mass. Measurements were separated into four periods, early light (07:00 to 13:00), late light (13:00 to 19:00), early dark (19:00 to 01:00), and late dark period (01:00 to 07:00), to distinguish between periods of high and low physical activity and were analyzed separately.

Glucose, Insulin, and Pyruvate Tolerance—Mice were fasted overnight; blood glucose levels and body weight (BW) were monitored before and after fasting. Subsequently, 2 g of D-glucose per kg of BW (glucose tolerance test), 0.75 units of insulin per kg of BW (insulin tolerance test), or 2 g of pyruvate per kg BW (pyruvate tolerance test) were intraperitoneally injected, and blood glucose levels were measured at indicated time points with an Accu-Check® Aviva glucose monitor (Roche Applied Science).

Insulin Signaling—Mice were fasted overnight and sedated with phenobarbital (180 mg/kg BW). Insulin (1 unit/kg BW) was injected directly into the vena cava inferior. Ten minutes after injection, the liver was removed, and fragments were snap-frozen in liquid nitrogen. After homogenization in a buffer supplemented with protease inhibitors, 1 mM NaF and 1 mM Na_3VO_4, Western blotting was performed using pan-AKT and phospho-AKT antibodies (Cell Signaling Technology).

Protein Analysis

Western Blotting—Western blotting experiments were conducted as described previously (17). Detection was performed using HRP-labeled secondary antibodies and ECL plus detection kit (Amersham Biosciences). Primary antibodies for ACC, pACC (Ser-79), AMPK, pAMPK (Thr-172, 40H9), Akt (pan, C67E7), pAkt (Ser-473, D9E), CREB (D76D11), and pCREB (Ser-133 D1G6) were purchased from Cell Signaling Technology, PGC-1α and SIRT1 antibodies were purchased from Santa

[2] The abbreviations used are: PPARα, peroxisome proliferator activated receptor α; AMPK, AMP-activated protein kinase; CREB, cAMP-response element-binding protein; F2,6BP, fructose 2,6-bisphosphate; G-6-Pase, glucose-6-phosphatase; PEPCK, phosphoenolpyruvate carboxykinase; PDH, pyruvate dehydrogenase complex; qRT, quantitative RT; BW, body weight; PAS, periodic acid-Schiff; ACC, acetyl-CoA carboxylase.

Cruz Biotechnology, and another PGC-1α antibody was purchased from Calbiochem. Analysis of PGC-1α acetylation was performed as described previously (18). The CRTC2 antiserum was used as described previously (19, 20). Band intensity was quantified with ImageMaster 1D.

Enzymatic Assays—Phosphoenolpyruvate carboxykinase (PEPCK) activity was determined as described previously (21, 22). Glucose-6-phosphatase (Glc-6-Pase) activity was measured by quantifying the release of phosphate from glucose 6-phosphate by an adapted method of Fiske-SubbaRow (see 23). Pyruvate dehydrogenase (PDH) activity was quantified using a PDH enzyme activity kit (MitoSciences) according to the manufacturer's guidelines.

Metabolic Analysis

Plasma Insulin Levels—Plasma insulin concentrations were determined using a commercial ELISA kit (Mercodia).

Glycogen Analysis—Aliquots of liver, homogenized in 0.06 N HCl, were spotted on Whatman paper and hydrolyzed with amyloglucosidase as described before (24). The amount of glucose released was quantified spectrophotometrically at 511 nm by a coupled glucose oxidase/peroxidase indicator reaction using 16 units of peroxidase, glucose oxidase (0.08 μg), 8 mM 2,4,2-tribromo-3-hydroxybenzoic acid, 2 mM 4-aminoantipyrine, and 0.02% Triton X-100 in a 0.1 M potassium phosphate buffer, pH 7, during 30 min at 25 °C (25). The distribution of glycogen in liver was visualized by PAS staining on formalin-fixed tissues.

Determination of ATP/AMP—Liver ATP and AMP levels were measured using ion-pair RP-HPLC (26). In short, livers were homogenized in ice-cold 0.4 M perchloric acid. External AMP and ATP standards were dissolved in 0.4 M perchloric acid and treated in the same way as the samples. After 10 min of centrifugation at 13,000 × *g*, the supernatant was neutralized with K_2CO_3. Perchlorate precipitates were removed by centrifugation, and the supernatant was injected on a 4.6 × 150-mm, 5-μm particle size C-18 HPLC column (Symmetry) at a rate of 1 ml/min, 100% buffer A from 0 to 5 min, 100% buffer A to 100% buffer B from 5 to 20 min, 100% buffer B from 20 to 31 min for column re-equilibration (buffer A: 25 mM NaH_2PO_4, 0.385 mM tetrabutylammonium, pH 5; buffer B: 10% (v/v) acetonitrile in 200 mM NaH_2PO_4, 0.385 mM tetrabutylammonium, pH 4). Phosphorylated nucleotides were monitored at 260 nm. Hepatic AMP and ATP content were quantified by comparison with external standards.

Determination of NAD^+/NADH—Cellular NAD^+ and NADH levels were quantified using an EnzyChrom™ NAD^+/NADH assay kit of Bioassay Systems (Hayward, CA) according to the manufacturer's guidelines. For 20 mg of liver, 400 μl of extraction buffer and 80 μl of assay buffer was used.

Fructose-2,6-bisphosphate—Hepatic levels of fructose-2,6-bisphosphate were quantified as described (27).

Analysis in Primary Hepatocytes

Hepatocyte Isolation—Hepatocytes were isolated as described previously (28) and seeded at 0.15 million cells/cm^2. For some experiments, hepatocytes were infected with adenovirus expressing PGC-1α (derived from Addgene plasmid 14426) (29) and with control adenovirus (30 pfu/cell) or treated with the AMPK inhibitor compound c (10 μM).

Glucose Secretion—1.5 million hepatocytes were seeded in a 6-well plate. After overnight culture, hepatocytes were maintained in glucose-free medium supplemented with 2 mM pyruvate and 20 mM lactate for 6 h. Glucose levels in the medium were quantified by a coupled glucose oxidase/peroxidase indicator reaction as described above (25). For normalization purposes, hepatocytes were harvested in homogenization buffer (0.05 M sodium phosphate buffer, 2.0 M NaCl, 2 mM EDTA, pH 7.4), and DNA content was determined by measuring fluorescence after incubation with Hoechst 33258 (1.6 μM) using a Fluostar fluorimeter (excitation at 355 nm and emission at 460 nm).

Glycolytic Flux—Glycolysis was measured as described previously (30). In short, 0.3 million hepatocytes were seeded in a 24-well plate. After overnight culture, cells were treated with [5-^{3}H]glucose (80 μCi/mmol glucose) for 6 h. The medium was collected in a glass vial, and the released ^3H, which was captured after 48 h at 37 °C on a H_2O-soaked filter paper in a plastic hanging well, was quantified by liquid scintillation counting.

RNA Analysis

Quantitative RT-PCR—qRT-PCR was performed as described previously using the primers listed in supplemental Table 1 and 5′-6-carboxyfluorescein- and 3′-tetramethyl-6-carboxyrhodamine-labeled probes (31). Relative expression levels of the target genes were calculated as a ratio to the reference gene β-actin.

Microarray Analysis—The transcriptional profiles of livers of 10-week-old wild type and *L-Pex5*$^{-/-}$ mice ($n = 3$) were analyzed using the whole genome Affymetrix GeneChip® mouse genome 430 2.0 array as described previously (31). Labeling of the samples, hybridization, washing, and scanning of the chips was carried out at the MicroArray Facility (Leuven, Belgium). Bioinformatic analysis was performed as described previously (31). The complete dataset is available under GEO record GSE27720.

Statistics—Results obtained in two groups of mice were compared by using the unpaired *t* test.

RESULTS

L-Pex5 Knock-out Mice Ingest More Food in Order to Remain Normoglycemic—To investigate whether loss of peroxisomal function in hepatocytes impacts carbohydrate homeostasis, blood glucose and insulin levels were determined. Glycemia and plasma insulin levels of *L-Pex5*$^{-/-}$ mice were not different from wild type mice in *ad libitum* fed as well as in 24-h fasted conditions (Table 1). When a bolus of glucose was injected in overnight fasted mice, glycemic response was comparable with that in control mice (data not shown). However, we noticed that food intake per gram of body weight was significantly higher in *L-Pex5*$^{-/-}$ mice compared with controls (155% of control mice) (Table 1). Notably, after pair feeding with control mice, blood glucose levels in *L-Pex5*$^{-/-}$ mice were significantly lower as compared with controls (Table 1). This was accompanied by severe weight loss, averaging 18% after 1 week and 27% after 4 weeks of pair feeding.

TABLE 1

General metabolic characteristics of *L-Pex5* knock-out and wild type mice in different nutritional conditions

Values are given as means ± S.E., $n = 4$ (plasma insulin), or $n \geq 8$; *L-Pex5*$^{-/-}$ *versus* control mice. Comparisons are as follows: ***, $p < 0.001$; **, $p < 0.01$; *, $p < 0.05$. NS means not significant; ND means not determined.

	Fed			24-h fasted			4 weeks pair fed	
	Ct	*L-Pex5*$^{-/-}$		*Ct*	*L-Pex5*$^{-/-}$		*L-Pex5*$^{-/-}$	
Body weight (g)	39.4 ± 0.8	31.0 ± 0.7	***	36.5 ± 2.0	27.7 ± 1.0	***	21.2 ± 1.4	***
Food intake (g/g lean mass)	1.0 ± 0.2	1.5 ± 0.2	***					
BW change 24-h fasted (% BW)				13 ± 0.8	17 ± 0.6	***	15 ± 0.9	NS
Plasma glucose (mg/dl)	122 ± 5	124 ± 3	NS	85 ± 4	77 ± 4	NS	106 ± 3	***
Plasma insulin (ng/ml)	2.2 ± 0.4	1.8 ± 0.2	NS	3.0 ± 1.5	1.1 ± 0.2	NS	ND	
Liver weight (% BW)	5.3 ± 0.2	9.5 ± 0.2	***	3.8 ± 0.2	7.6 ± 0.2	***	7.8 ± 0.1	***

To relate the increased food consumption to energy expenditure, indirect calorimetry studies were performed in *L-Pex5*$^{-/-}$ ($n = 7$) and control mice ($n = 7$) for a period of 5 consecutive days under *ad libitum* fed conditions. Energy expenditure levels were significantly higher in *L-Pex5*$^{-/-}$ mice compared with controls during all time periods (Fig. 1*A*). Respiratory exchange rates did not differ between groups during any of the periods measured indicating that relative substrate selection did not differ between groups (Fig. 1*B*). The higher energy expenditure levels were reflected in a significantly higher absolute rate of carbohydrate oxidation in *L-Pex5*$^{-/-}$ mice during the late light period, early dark period, and late dark period (Fig. 1*C*). In addition, absolute carbohydrate oxidation rates during the early light period tended to be higher in *L-Pex5*$^{-/-}$ mice compared with controls, although this did not reach levels of statistical significance ($p = 0.056$). Absolute fat oxidation rates did not differ between groups during any of the periods measured (Fig. 1*D*). Although calorimetry studies were not repeated under fasted conditions, we obtained indirect evidence for increased fat oxidation in *L-Pex5*$^{-/-}$ mice as compared with controls during fasting or when fed a high fat diet by monitoring body weights and fat pads (32). These data demonstrate that *L-Pex5*$^{-/-}$ mice have a higher metabolic rate compared with control mice. Taken together, *L-Pex5*$^{-/-}$ mice ingest more food to compensate for increased energy expenditure, but are able to maintain normoglycemia in *ad libitum* fed and in fasted conditions.

Loss of Functional Peroxisomes Alters Expression of Genes Involved in Carbohydrate Metabolism—To get a broad overview of deregulated metabolic pathways in livers of *L-Pex5*$^{-/-}$ mice, microarray analysis was performed on mice in the fed state. As summarized in Table 2, substantial up- and down-regulation was observed in genes involved in gluconeogenesis, glycogen synthesis, and signaling pathways that regulate metabolic homeostasis. To examine the physiological impact of the metabolic gene deregulation, *in vivo* and *in vitro* experiments were conducted. The hepatic phenotype was evaluated under basal conditions and following 24 h fasting, a stimulus known to induce fatty acid oxidation and gluconeogenesis in liver.

Glycolysis Is Enhanced in Peroxisome-deficient Livers—We previously reported that in peroxisome-deficient livers activities of the glycolytic enzymes glucokinase and pyruvate kinase were increased (11).

To investigate whether this resulted in increased conversion of glucose into pyruvate, glycolytic flux experiments were conducted in cultured hepatocytes. The production of ^3H_2O from [5-^{3}H]glucose was 3.3-fold increased in peroxisome-deficient as compared with control hepatocytes (183 *versus* 55 nmol/h/10^6 cells; Fig. 1*E*). According to the present microarray data, the mRNA levels encoding glucokinase, the first enzyme of the pathway, and phosphofructokinase-1, the rate-limiting enzyme, were unaltered in livers of *L-Pex5*$^{-/-}$ mice (Table 2). Unaltered mRNA levels of glucokinase, 6-phosphofructo-2-kinase/fructose-2,6-biphosphatase 3 (PFKFB3), and lactate dehydrogenase (LDH) were also confirmed by qRT-PCR analysis (data not shown). Expression levels of aldolase A, however, were 2-fold increased (Table 2). To assess alternative control mechanisms, we measured the levels of fructose 2,6-bisphosphate (F2,6BP), which is a crucial allosteric stimulator of phosphofructokinase 1 (PFK1), and hence of the entire glycolytic pathway. However, levels of F2,6BP were not elevated in peroxisome-deficient livers (data not shown). Thus, glycolytic induction likely occurs at least partly via post-transcriptional or post-translational mechanisms (see below).

The PDH controls the entry of glycolytic intermediates into the TCA cycle. In line with the increased glycolytic flux, the PDH activity was also significantly higher in *L-Pex5*$^{-/-}$ mice (Fig. 1*F*). A family of kinases inactivates this PDH complex, thereby preventing the entry of pyruvate in the Krebs cycle and mitochondrial ATP production from glucose. Expression levels of PDK2, the most abundant pyruvate dehydrogenase kinase isoform in liver, were not altered in *L-Pex5*$^{-/-}$ mice (data not shown), whereas PDK4 transcripts were 8.6-fold up-regulated (Table 2). Thus, despite up-regulation of PDK4, PDH activity was increased, implying that regulation of PDH activity in *L-Pex5*$^{-/-}$ mice is complex and likely requires additional post-transcriptional mechanisms (see below).

Gluconeogenesis Is Impaired in Peroxisome-deficient Livers—The mRNA levels of two key enzymes of gluconeogenesis *Pck1* encoding PEPCK, which is involved in the early steps, and *G6pc* encoding glucose-6-phosphatase (G-6-Pase), which is involved in the terminal step, were suppressed in the fed state according to microarray analysis (Table 2). Activities of these gluconeogenic enzymes were correspondingly reduced reaching 76% of control levels for PEPCK (Fig. 2*A*) and 36% for G-6-Pase (Fig. 2*B*). Upon fasting, mRNA levels of *Pck1* increased in both genotypes, indicating a normal response to food deprivation, but they remained lower in *L-Pex5*$^{-/-}$ mice, as quantified by qRT-PCR (data not shown). Expression of the glucose 6-phosphate transporter that couples with G-6-Pase to form an active G-6-Pase complex in the endoplasmic reticulum membrane was reduced to 25% of control values and expression of SLC2a2 (glucose transporter 2, GLUT2), the transporter that exports glucose, to 37% (Table 2).

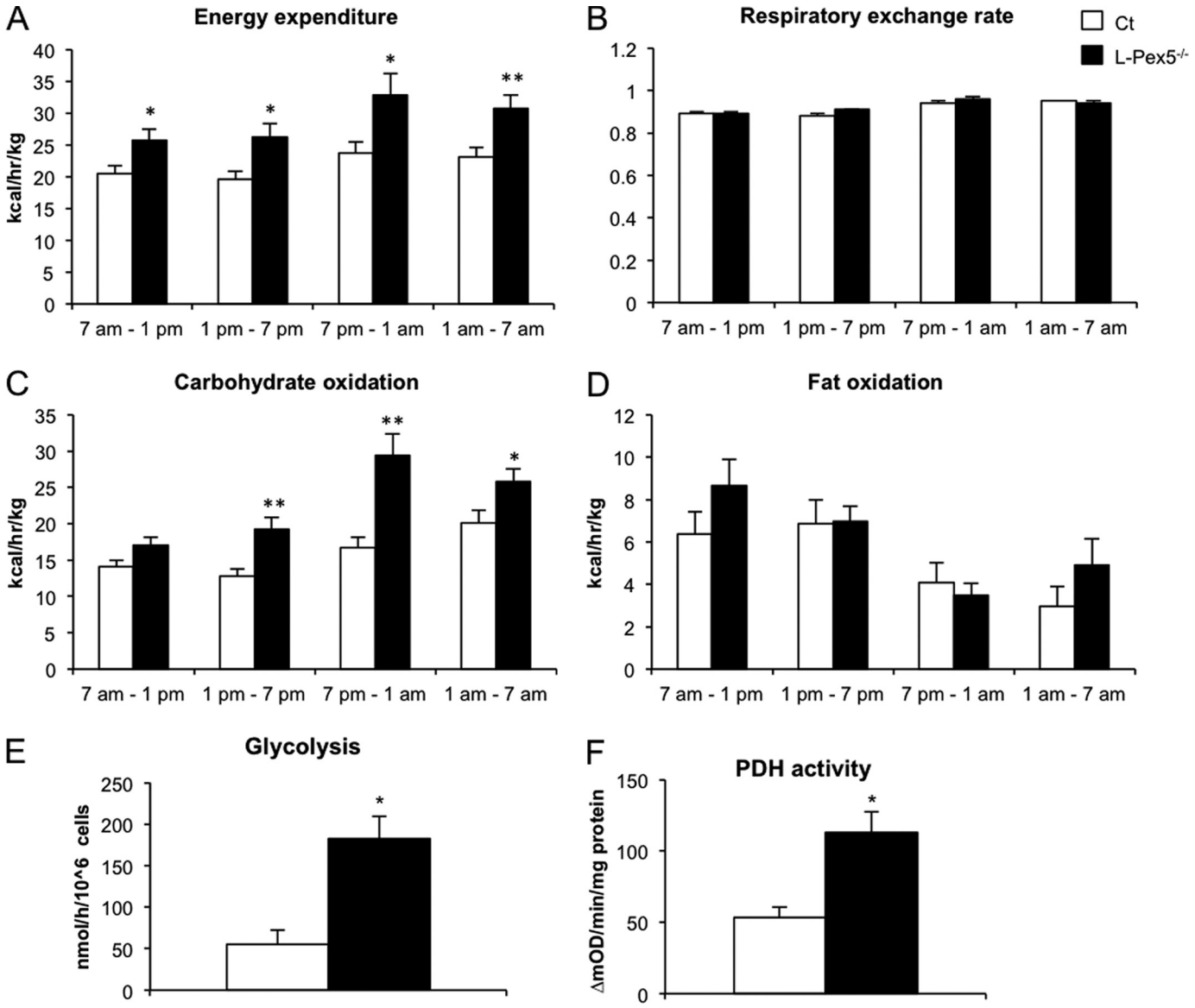

FIGURE 1. **Utilization of carbohydrates is increased upon hepatic peroxisome deficiency *in vivo* and *in vitro*.** *L-Pex5*$^{-/-}$ and control mice were subjected to indirect calorimetry measurements for a period of 5 consecutive days ($n = 7$). Energy expenditure (*A*), respiratory exchange rate (*B*), carbohydrate oxidation (*C*), and fat oxidation (*D*) are shown. *E*, glycolytic flux was significantly increased in primary *Pex5*$^{-/-}$ hepatocytes (shown as nanomoles of glucose/h/10^6 cells) ($n = 4$). *F*, PDH activity (shown as ΔmOD/min/mg protein) was strongly increased in liver homogenates of fed *L-Pex5*$^{-/-}$ mice ($n = 4$). Values are given as means ± S.E. *L-Pex5*$^{-/-}$ *versus* control mice or hepatocytes: **, $p < 0.01$; * $p < 0.05$.

To test whether this reduced expression/activity of hepatic gluconeogenic enzymes impaired whole body glucose synthesis, a pyruvate tolerance test was performed. Following pyruvate injection, the maximum blood glucose levels that were reached were significantly lower in *L-Pex5*$^{-/-}$ mice as compared with control mice (Fig. 2*C*). We further confirmed that the glucose output capacity of peroxisome-deficient hepatocytes was reduced by incubating isolated hepatocytes in a glucose-free medium supplemented with lactate and pyruvate. Glucose secretion from *Pex5*-deficient hepatocytes was reduced by 19% (Fig. 2*D*).

Expression levels of several key enzymes of the pentose phosphate pathway were examined in the microarray data. Only transketolase was induced in *L-Pex5*$^{-/-}$ mice, whereas transcripts from other enzymes were unaltered (Table 2).

Glycogen Synthesis Is Impaired in L-Pex5 Knock-out Mice—The mRNA levels of glycogen synthase 2 (*Gys2*), the rate-limiting enzyme of hepatic glycogen synthesis, were markedly reduced in *L-Pex5* knock-out mice (40 and 33% of control as determined by microarray (Table 2) and qRT-PCR (Fig. 3*A*), respectively). The expression of glycogen synthase kinase 3β (*Gsk3*β), which inactivates GYS2, was concomitantly increased at the mRNA (165% of control, Table 2) and at the protein level (data not shown), also pointing to an impaired glycogen synthesis. Hepatic glycogen stores, measured enzymatically in *ad libitum* fed mice, were significantly reduced (59% of control levels) (Fig. 3*B*). This was confirmed by PAS staining, which also revealed that glycogen was more evenly distributed in *L-Pex5*$^{-/-}$ livers compared with the more pronounced periportal staining in control mice (Fig. 3*C*). After a 24-h fasting

TABLE 2

Microarray analysis on livers of *L-Pex5* knock-out and wild type mice (aged 20 weeks, $n = 3$)

Hepatic expression levels of important genes in carbohydrate metabolism are shown. Comparisons of *L-Pex5*$^{-/-}$ *versus* control mice are as follows: ***, $p < 0.001$; **, $p < 0.01$; *, $p < 0.05$.

Symbol	Description	Fold change	Pathway
Gck	Glucokinase	0.97	Glycolysis
Khk	Ketohexokinase	0.45***	
Pfkl	Phosphofructokinase, liver, B-type	0.90	
Aldoa	Aldolase 1, A isoform	2.04***	
Aldob	Aldolase 2, B isoform	1.06	
Gapdh	Glyceraldehyde-3-phosphate dehydrogenase	1.02	
Pklr	Pyruvate kinase liver and red blood cell	0.76*	
Pdk4	Pyruvate dehydrogenase kinase, isoenzyme 4	8.57**	
G6pc	Glucose-6-phosphatase, catalytic	0.55*	Gluconeogenesis
Pck1	Phosphoenolpyruvate carboxykinase 1, cytosolic	0.28***	
Slc2a2	Solute carrier family 2 (facilitated glucose transporter), member 2 = Glut2	0.37***	
Slc37a4	Solute carrier family 37 (glucose-6-phosphate transporter), member 4 = G6PT	0.25***	
Pcx	Pyruvate carboxylase	0.84*	
Fbp1	Fructose bisphosphatase 1	1.17	
Fbp2	Fructose bisphosphatase 2	2.39***	
Gyk	Glycerol kinase	0.89	
Gys2	Glycogen synthase 2	0.41***	Glycogen
Pygl	Liver glycogen phosphorylase	0.60***	
Gsk3b	Glycogen synthase kinase 3β	1.68**	
Slc2a2	Solute carrier family 2 (facilitated glucose transporter), member 2	0.37***	
Tkt	Transketolase	1.52***	PPP
Taldo1	Transaldolase 1	1.01	
Rpe	Ribulose-5-phosphate-3-epimerase	0.97	
G6pd2	Glucose-6-phosphate dehydrogenase 2	0.95	
G6pdx	Glucose-6-phosphate dehydrogenase X-linked	1.07	
Akt2	Thymoma viral proto-oncogene 2 (insulin target tissues: liver, fat, muscle)	0.72***	Insulin signaling
Irs1	Insulin receptor substrate 1	0.61*	
Irs2	Insulin receptor substrate 2	1.00	
Srebf1	Sterol regulatory element-binding factor 1 = SREBP 1c	0.46***	
Trib3	Tribbles homolog 3 (*Drosophila*)	25.5***	
Appl1	Adaptor protein, phosphotyrosine interaction, pleckstrin homology domain, and leucine zipper containing 1	1.30	
Pten	Phosphatase and tensin homolog	0.89**	
Stat3	Signal transducer and activator of transcription 3	0.73**	
Ppargc1a	Peroxisome proliferative-activated receptor γ, coactivator 1α	0.30***	Regulatory genes
Creb1	cAMP-responsive element-binding protein 1	1.18	
Crebbp	CREB-binding protein	1.26**	
Crtc2	CREB-regulated transcription coactivator 2	0.74**	
Hnf4a	Hepatic nuclear factor 4, α	1.41	
Foxo1	Forkhead box O1	0.75**	
Prkaca	Protein kinase, cAMP-dependent, catalytic, α = PKA	0.83*	
Snf1lk	SNF1-like kinase = SIK	1.02	
Clk2	CDC-like kinase 2	1.25	
Ncoa1	Nuclear receptor coactivator 1 = Src1	1.13	
Ncoa3	Nuclear receptor coactivator 3 = Src3	0.93	
Gcn5l2	GCN5 general control of amino acid synthesis-like 2 (yeast)	1.56***	
Cdk9	Cyclin-dependent kinase 9 (CDC2-related kinase)	1.62***	
Prmt1	Protein arginine *N*-methyltransferase 1	1.32*	
Sirt1	Sirtuin 1 ((silent mating type information regulation 2, homolog) 1 (*Saccharomyces cerevisiae*)	1.11	
Mapk14	Mitogen-activated protein kinase 14 = p38 MAPK	0.78**	
Prkaa1	Protein kinase, AMP-activated, α1 catalytic subunit = AMPKa1	1.34*	
Prkaa2	Protein kinase, AMP-activated, α2 catalytic subunit = AMPKa2	1.64**	
Cebpa	CCAAT/enhancer-binding protein (C/EBP), α	0.79*	
Mlxipl	MLX interacting protein-like = chrebp	1.12	
Thra	Thyroid hormone receptor α	0.86	
Thrb	Thyroid hormone receptor β	0.58**	
Atf3	Activating transcription factor 3	10.1***	Endoplasmic reticulum stress
Atf4	Activating transcription factor 4	1.72***	
Atf6	Activating transcription factor 6	1.63***	
Ddit3	DNA-damage inducible transcript 3 = CHOP	5.18***	
Ern2	Endoplasmic reticulum (ER) to nucleus signaling 2 = IRE1	0.89	
Eif2ak3	Eukaryotic translation initiation factor 2 α kinase 3 = PERK	1.49**	
Xbp1	X-box-binding protein 1	0.72**	
Hspa5	Heat shock protein 5 = GRP78	0.78*	
Eif2a	Eukaryotic translation initiation factor 2a	1.18*	
Calr	Calreticulin	0.61***	
Canx	Calnexin	0.86	
Asns	Asparagine synthetase	4.74*	
Herpud1	Homocysteine-inducible, endoplasmic reticulum stress-inducible, ubiquitin-like domain member 1	0.58	
Edem1	ER degradation enhancer, mannosidase α-like 1	0.81	

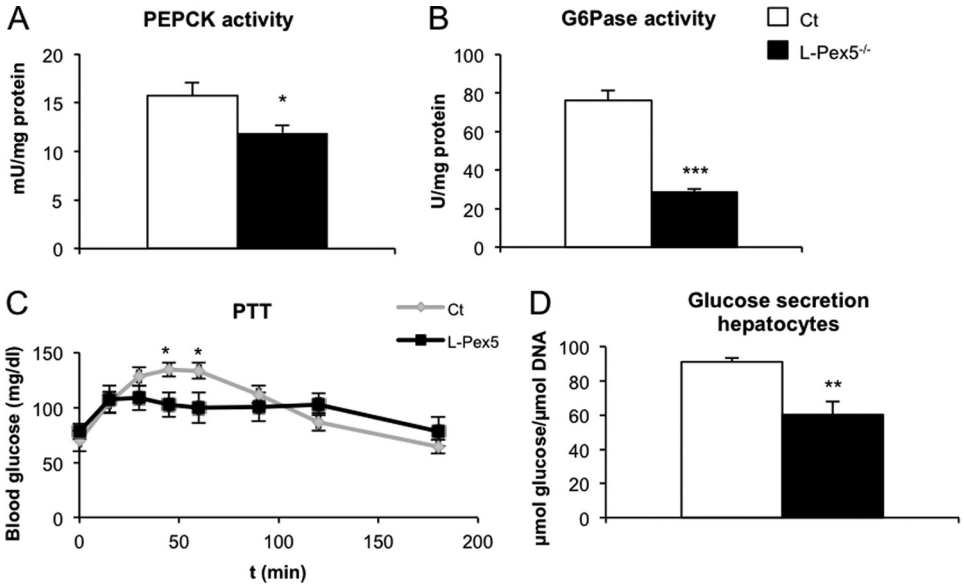

FIGURE 2. **Gluconeogenesis is suppressed in *L-Pex5*$^{-/-}$ mice.** PEPCK activity (shown as milliunits/mg protein) (*A*) and G-6-Pase activity (shown as units/mg protein) (*B*) were significantly lower in liver homogenates of fed *L-Pex5*$^{-/-}$ mice ($n = 4$). *C*, pyruvate tolerance test (*PTT*): following a bolus injection of pyruvate, plasma glucose levels were measured at the indicated time points ($n = 7$). Maximal values reached were significantly lower in *L-Pex5*$^{-/-}$ mice. *D*, glucose secretion by primary hepatocytes was suppressed in *Pex5*$^{-/-}$ hepatocytes ($n = 4$). Data were normalized for DNA content. All values are given as means ± S.E. *L-Pex5*$^{-/-}$ *versus* control mice: ***, $p < 0.001$; **, $p < 0.01$; *, $p < 0.05$.

period, glycogen stores were depleted to the same extent in control and *L-Pex5*$^{-/-}$ livers (Fig. 3*B*). Interestingly, a 5-h refeeding period following a 24-h fast was sufficient to replenish glycogen in control livers but not in *L-Pex5*$^{-/-}$ livers (30% of control levels) (Fig. 3*B*), pointing to a slower synthesis of glycogen, which was also confirmed by PAS staining (Fig. 3*C*).

Peroxisome-deficient Hepatocytes Are Insulin-resistant—Because insulin sensitivity is an import aspect of carbohydrate homeostasis, *L-Pex5*$^{-/-}$ mice were challenged with insulin, but there was no difference in glycemic profile with control mice (Fig. 4*A*). As skeletal muscle is the primary site of insulin-dependent glucose disposal, this tissue may mask defects in hepatic insulin sensitivity. Therefore, insulin signaling in the liver was studied by analysis of downstream AKT phosphorylation subsequent to the injection of a bolus of insulin. As shown in Fig. 4, *B* and *C*, pAKT levels were significantly lower in *L-Pex5*$^{-/-}$ as compared with control mice. It should be noted that according to microarray analysis and Western blotting, expression levels of AKT were reduced to 81 and 61% of wild type levels, respectively. Together, it appears that peroxisome-deficient hepatocytes are markedly insulin-resistant, which, at first sight, is difficult to reconcile with reduced gluconeogenesis.

Acute Elimination of Peroxisomes Causes Similar Perturbations of Carbohydrate Metabolism but No Insulin Resistance—To investigate whether the observed deregulation of carbohydrate metabolism required a long term adaptation to the absence of functional hepatic peroxisomes, *Pex5* was acutely inactivated in the liver by intravenously injecting adenovirus-expressing CRE recombinase in *Pex5*$^{FL/FL}$ mice. Reduction of *Pex5* transcripts was confirmed by qRT-PCR, and only those mice with a reduction exceeding 90% were used for further analysis (Fig. 5*A*). Two weeks after injection, expression of *Pck1*, *Slc2a2* (encoding GLUT2), and *Gys2* was decreased to a similar extent as in livers of *L-Pex5*$^{-/-}$ mice (Fig. 5*B*), and GSK3β protein levels were increased (data not shown). This suppression of Gys2 and induction of GSK3β resulted in depleted hepatic glycogen stores (Fig. 5*C*). In contrast, however, in *adeno-Cre-Pex5* mice, insulin sensitivity determined by quantifying pAKT levels did not show any difference with control virus-injected mice (data not shown). Thus, alterations in carbohydrate metabolism occur rapidly after the disappearance of peroxisomes, whereas insulin resistance only arises after prolonged peroxisome inactivation in hepatocytes.

Alterations in Carbohydrate Metabolism Are Not Dependent on PPARα Activation—To explore the mechanisms underlying the deregulated carbohydrate metabolism in peroxisome-deficient liver, a number of key switches of energy homeostasis were investigated.

Among the most striking data of the microarray analysis was the significant induction of an array of PPARα target genes (32). This confirmed our previous observations using Northern blot analysis (11), and it is indicative of the accumulation of PPARα ligands in *L-Pex5*$^{-/-}$ livers, likely a consequence of the inactive peroxisomal β-oxidation. Several of these strongly induced PPARα target genes are involved in lipid metabolism, but others have a distinct role in glucose homeostasis, such as PDK4 (see above) and TRIB3 (see below).

Because PPARα was previously shown to have a broad impact on several steps of carbohydrate metabolism (33), we investigated whether carbohydrate deregulation in *L-Pex5*$^{-/-}$ mice could be in part the result of PPARα activation. We generated mice with peroxisome-deficient hepatocytes in a *Pparα* null background by injecting *Pex5*$^{FL/FL}$*Pparα*$^{-/-}$ mice with adenovirus encoding CRE recombinase. Surprisingly, however, qRT-PCR analysis 2 weeks later showed that expression levels of *Pck1*, *Slc2a2*, and *Gys2* were even more extensively decreased as compared with *Pex5*$^{FL/FL}$*Pparα*$^{+/+}$ mice treated with adeno-

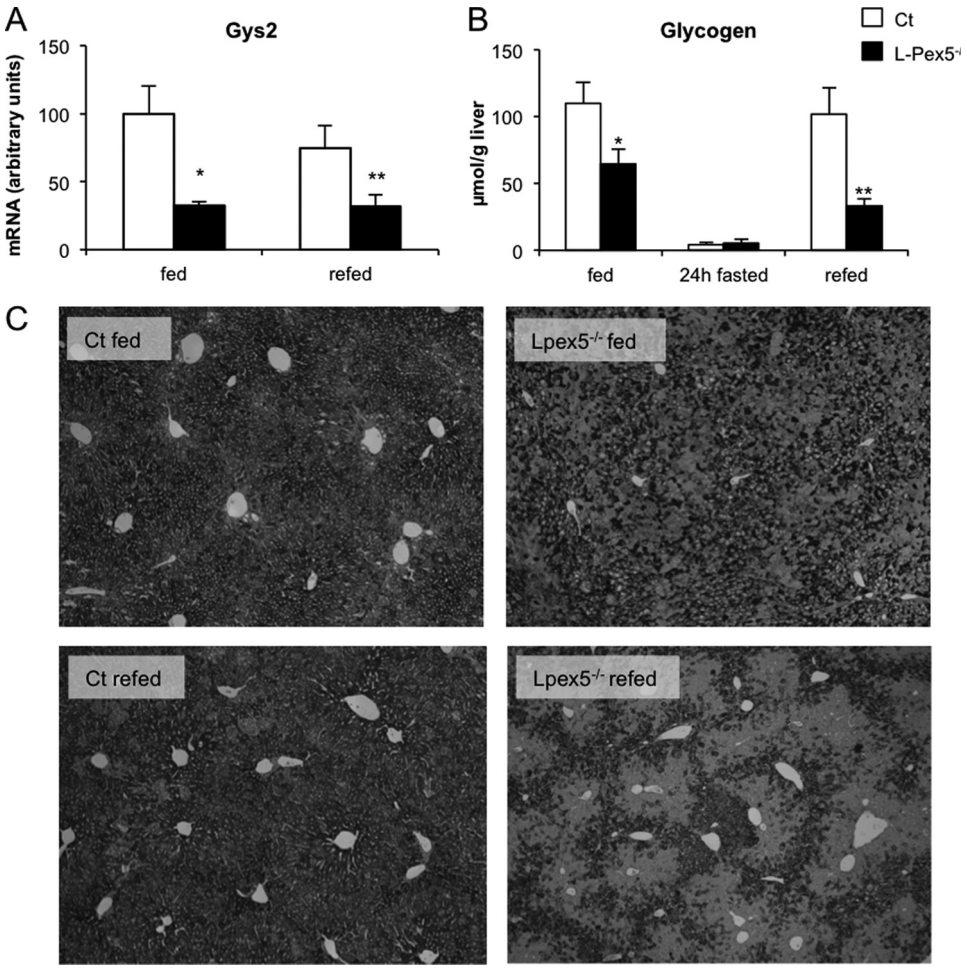

FIGURE 3. **Glycogen synthesis is suppressed in *L-Pex5*$^{-/-}$ mice.** *A,* hepatic gene expression levels of Gys2 were significantly reduced in *L-Pex5*$^{-/-}$ mice. Expression levels were normalized to β-actin expression. *B,* hepatic glycogen levels in fed, 24-h fasted, and 24-h fasted and 5-h refed mice shown as μmol/g liver. Glycogen stores were markedly reduced both in fed and in refed *L-Pex5*$^{-/-}$ mice. *C,* PAS staining of liver in fed and in 24-h fasted and 5-h refed mice. Glycogen was less abundant and more randomly distributed in fed *L-Pex5*$^{-/-}$ mice and glycogen stores were slower repleted upon refeeding following a 24-h fasting period in *L-Pex5*$^{-/-}$ mice. Values are given as means $\pm$ S.E., $n = 4$. *L-Pex5*$^{-/-}$ *versus* control mice: **, $p < 0.01$; *, $p < 0.05$.

viral CRE recombinase (Fig. 6, *A–C*). Thus, the observed impairment of gluconeogenesis and glycogen synthesis was independent of the activation of PPARα in *L-Pex5*$^{-/-}$ mice.

PPARα is a strong inducer of TRIB3, which suppresses insulin signaling during fasting by blocking activation of AKT. TRIB3 induction has been linked to the development of insulin resistance (34–36), although this effect is still debated because insulin sensitivity was normal in *Trib3*$^{-/-}$ mice (37) and upon TRIB3 overexpression in primary hepatocytes (38).

In agreement with the observed PPARα activation, qRT-PCR showed that *Trib3* expression levels were 41-fold increased in *L-Pex5*$^{-/-}$ mice and 8-fold in *adeno-Cre Pex5*$^{FL/FL}$*Ppar*$\alpha^{+/+}$ mice but, as expected, not in *adeno-Cre Pex5*$^{FL/FL}$*Ppar*$\alpha^{-/-}$ mice (data not shown). Thus, even though the 41-fold increase in *Trib3* levels in *L-Pex5*$^{-/-}$ mice might, at first sight, suggest that they could cause hepatic insulin resistance, the experiments with the acute inactivation of peroxisomes show that the 8-fold increase in *Trib3* expression did not suffice to induce insulin resistance. Therefore, it is unlikely that insulin resistance is due to a PPARα-mediated increase of Trib3 expression.

The Energy Sensor AMPK Is Activated in Peroxisome-deficient Hepatocytes—As we previously demonstrated that loss of functional peroxisomes in hepatocytes causes important mitochondrial impairment at the level of energy production via OXPHOS (11), we investigated whether the energy sensor AMPK might be involved. This kinase is activated by increased cellular AMP/ATP ratios, and it stimulates catabolic pathways and suppresses anabolic pathways to restore the cellular energy balance. AMP/ATP ratios were significantly increased in *L-Pex5*$^{-/-}$ mice (Fig. 7*A*), indicating that hepatocytes of *L-Pex5*$^{-/-}$ mice had an energy deficit. Via Western blot analysis, we quantified the levels of active phosphorylated AMPK (pAMPK) and the level of phosphorylation of its targets ACC (pACC) and GSK3β (pGSK3β). *L-Pex5*$^{-/-}$ mice showed significantly higher pAMPK levels and an even more marked increase of its targets, pACC and pGSK3β, as compared with control littermates (Fig. 7, *B–D*). The phosphorylated form of ACC, a key enzyme in lipogenesis, is inactive, which results in reduced generation of malonyl-CoA. This is in agreement with reduced lipid synthesis in *L-Pex5*$^{-/-}$ mice (32) and with increased fatty acid oxidation as has been observed both in primary hepatocytes (28) and *in vivo* (32).

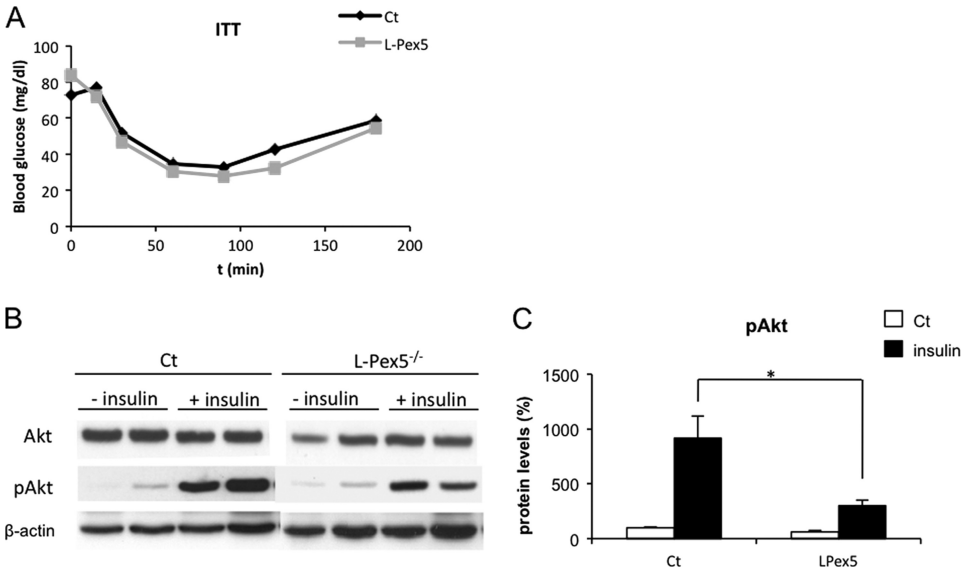

FIGURE 4. **Insulin signaling is impaired in *Pex5*$^{-/-}$ livers.** *A,* insulin tolerance test (*ITT*). *L-Pex5*$^{-/-}$ mice showed a normal blood glucose response upon injection of a bolus of insulin. *B* and *C, in vivo* insulin signaling. Western blot (*B*) and quantification of Western blot (*C*) of AKT and phosphorylated AKT (*pAKT*) 10 min after injection of insulin or vehicle. Levels of pAKT were lower in *Pex5*$^{-/-}$ liver after insulin stimulation. Values are given as means ± S.E., $n \geq 4$. *L-Pex5*$^{-/-}$ *versus* control mice *, $p < 0.05$.

Activated AMPK Contributes to the Deregulation of Carbohydrate Homeostasis in L-Pex5$^{-/-}$ *Mice*—One of the established mechanisms through which AMPK suppresses gluconeogenic gene expression is the phosphorylation and resultant nuclear exclusion of CRTC2 (also named TORC2), a transcriptional coactivator of cAMP- response element-binding protein (CREB) (20, 39–41). As a result, gene transcription of the key gluconeogenic genes PEPCK and G-6-Pase is repressed. To evaluate the contribution of activated AMPK to the suppressed gluconeogenesis in *L-Pex5*$^{-/-}$ mice, we studied CRTC2 phosphorylation and its subcellular localization in *L-Pex5*$^{-/-}$ livers. CRTC2 was significantly more phosphorylated, and thus inactive, in knock-out livers (Fig. 8*A*). In agreement, in the fasted state, the coactivator was sequestered in the cytosol of *L-Pex5*$^{-/-}$ hepatocytes, whereas it was located in the nucleus of control mice (Fig. 8*B*). Thus, CREB/CRTC2-mediated transcription of the gluconeogenic genes is likely suppressed in *Pex5*$^{-/-}$ hepatocytes.

Recently, it was reported that phosphorylation of GSK3β by AMPK is also an important path for the inhibitory effects of AMPK on PEPCK expression (42). As mentioned above, the phosphorylation status of GSK3β was indeed increased in *Pex5*-deficient hepatocytes (Fig. 7*D*).

To further study the role of activated AMPK in carbohydrate deregulation in *L-Pex5*$^{-/-}$ mice, we blocked its activity with compound c in primary hepatocyte cultures. First, we confirmed that the transcriptional alterations of gluconeogenic and glycogenic genes were conserved when *Pex5*$^{-/-}$ hepatocytes were cultured for up to 48 h (Fig. 8, *C–E,* and data not shown). Treatment with the AMPK inhibitor compound c restored expression levels of *Pck1*, *G-6-Pase*, *Gys2,* and *Slc2a2* (Fig. 8, *C–E* and data not shown). Inhibition of AMPK also decreased the glycolytic flux in *Pex5*$^{-/-}$ hepatocytes to wild type levels (Fig. 8*F*). Thus, AMPK contributes to the suppression of gluconeogenesis and glycogen synthesis and to the induction of glycolysis in *Pex5*-deficient hepatocytes.

PGC-1α Expression and Activity Are Suppressed—PGC-1α, a promiscuous transcriptional coactivator involved in the control of energy homeostasis, was down-regulated more than 3-fold according to the microarray analysis (Table 2). PGC-1α is a central regulator of hepatic gluconeogenesis and induces the enzymes PEPCK and G-6-Pase via coactivation of FOXO1, HNF4α, and the glucocorticoid receptor (43–46). Reduced mRNA expression of PGC-1α was confirmed by qRT-PCR in fed and fasted mice (Fig. 9*A* and data not shown) and by Western blot analysis after immunoprecipitation (Fig. 9*C*). Also acute deletion of *Pex5* by adenoviral Cre recombinase in *Pex5*$^{FL/FL}$ mice triggered a strong down-regulation of PGC-1α (Fig. 9*A*), which also occurred in a PPARα-deficient background (data not shown), again illustrating that the observed metabolic changes occur independently of PPARα.

To investigate the origin of the markedly reduced PGC-1α transcripts, we examined whether the known inducer of PGC-1α, activated CREB, was affected in peroxisome-deficient livers. Remarkably, phosphorylated CREB was indeed significantly reduced in *L-Pex5*$^{-/-}$ mice, but this was not the case in *adeno-Cre-Pex5* mice (Fig. 9*B*). Thus, reduced signaling through pCREB cannot be the only cause of PGC-1α suppression.

The activity of PGC-1α strongly depends on post-translational modifications, of which reversible acetylation is the most important. SIRT1 deacetylates and activates PGC-1α, whereas GCN5 acetylates and deactivates the coactivator. To determine the acetylation status, Western blots of immunoprecipitated PGC-1α were stained with acetyl-lysine antibody. The relative acetylation state of PGC-1α was increased in *L-Pex5*$^{-/-}$ mice based on strongly reduced PGC-1α protein levels and equal levels of acetylated PGC-1α in control and knock-out livers (Fig. 9*C*). In agreement, levels of the NAD^+-dependent deacetylase SIRT1 were significantly decreased in *L-Pex5*$^{-/-}$ mice (26% of levels in fed control mice) (Fig. 9*D*). Furthermore, in view of the impaired oxidative phosphorylation (11), which may lower the redox state, we quantified NAD^+ and NADH

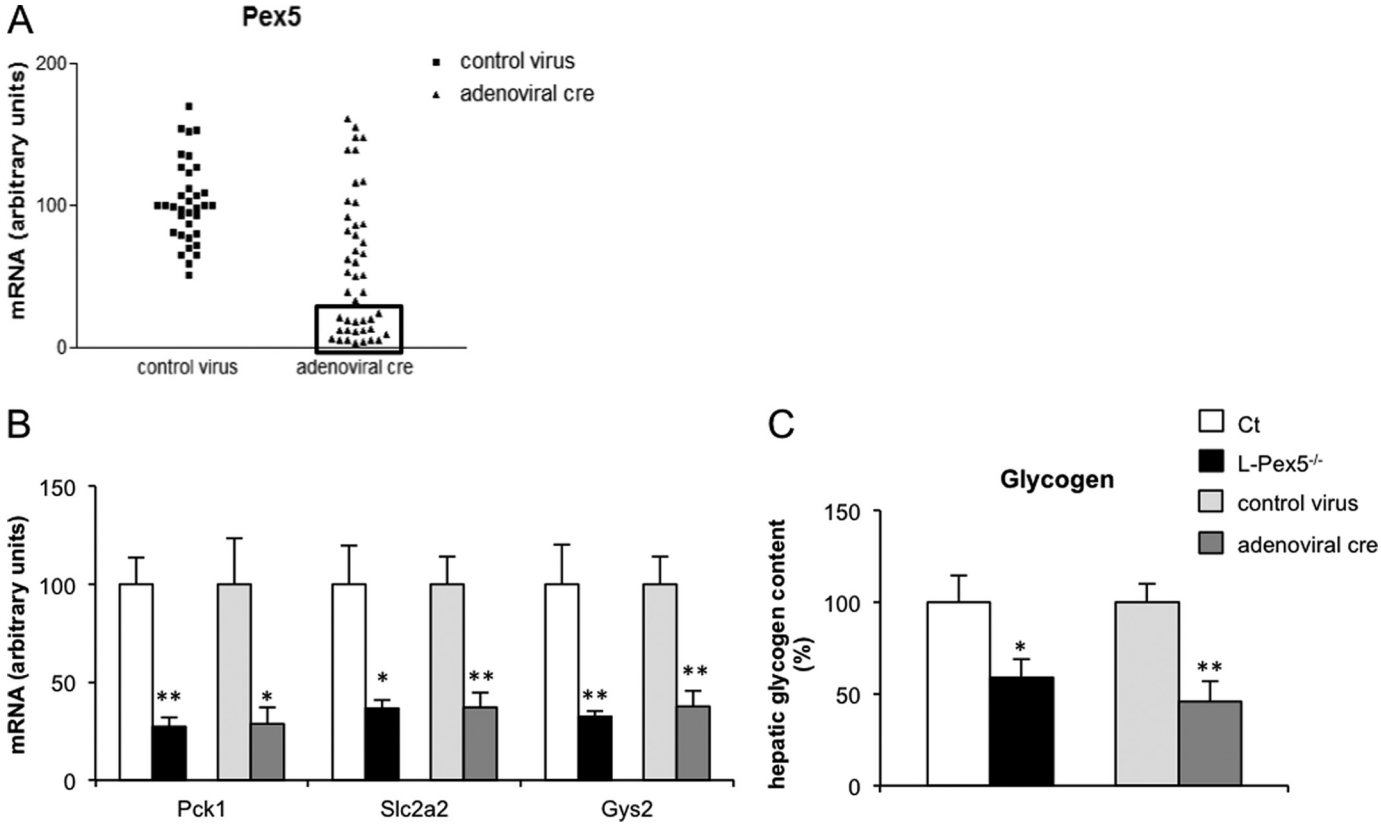

FIGURE 5. **Impaired gluconeogenesis and glycogen synthesis after acute elimination of functional peroxisomes.** Adeno-Cre or control adenovirus was administered to *Pex5*$^{FL/FL}$ mice, and mice were analyzed after 2 weeks. *A,* hepatic gene expression levels of *Pex5* normalized to *β-actin* expression. Individual data are plotted, and only those mice with <10% of *Pex5* mRNA levels (framed data points) were further analyzed. Hepatic gene expression levels of *Pck1*, *Slc2a2*, and *Gys2* normalized to *β-actin* expression (*B*) and hepatic glycogen levels (*C*) in control virus and adeno-Cre virus injected *Pex5*$^{FL/FL}$ mice are compared with those in *L-Pex5*$^{-/-}$ mice. Values are given as means ± S.E., $n = 4$. Control virus *versus* adeno-Cre virus-injected *Pex5*$^{FL/FL}$ mice: **, $p < 0.01$; *, $p < 0.05$.

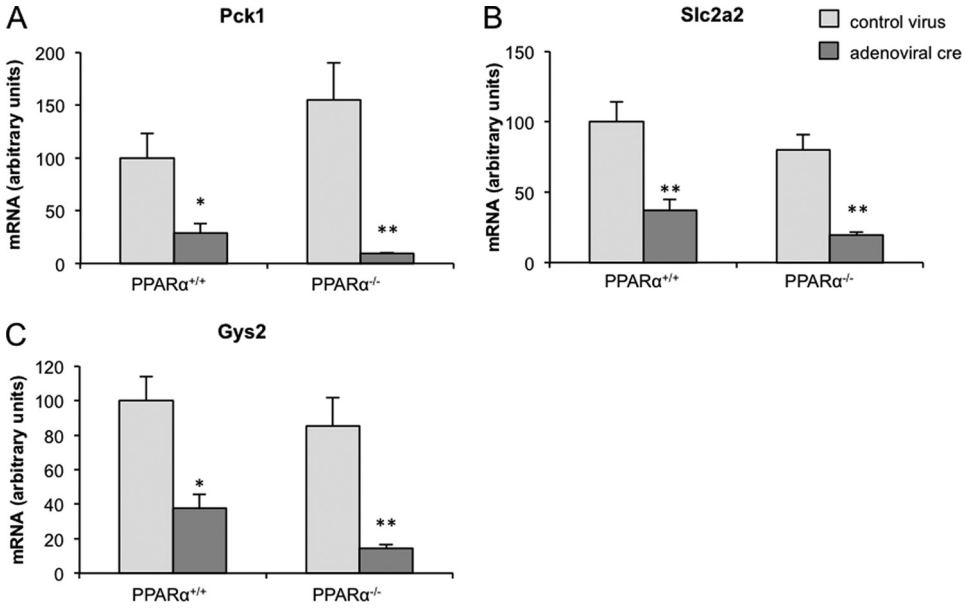

FIGURE 6. **Deregulation of carbohydrate metabolism in peroxisome-deficient liver is independent of PPARα activation.** Glucose metabolism in *Pex5*$^{FL/FL}$*Ppar*$\alpha^{+/+}$ mice and *Pex5*$^{FL/FL}$*Ppar*$\alpha^{-/-}$ mice, 14 days after administration of adenoviral Cre recombinase or control virus, is shown. Hepatic gene expression levels of *Pck1*, *Slc2a2*, and *Gys2* are shown. Expression levels were normalized to *β-actin* expression, and values are given as means ± S.E. for $n = 4$. In the absence of PPARα, deletion of *Pex5* caused even stronger down-regulation of gluconeogenic and glycogenic genes. Control virus *versus* adeno-Cre virus injected mice: **, $p < 0.01$; *, $p < 0.05$.

levels in liver homogenates. Interestingly, the cellular NAD^+/NADH ratio was significantly decreased in peroxisome-deficient livers (Fig. 9*E*), likely contributing to reduced SIRT1 activity. Finally, mRNA levels of GCN5, which acetylates and thereby inactivates PGC-1α, were increased in *L-Pex5*$^{-/-}$ mice (Table 2). Thus, both expression and function of PGC-1α are

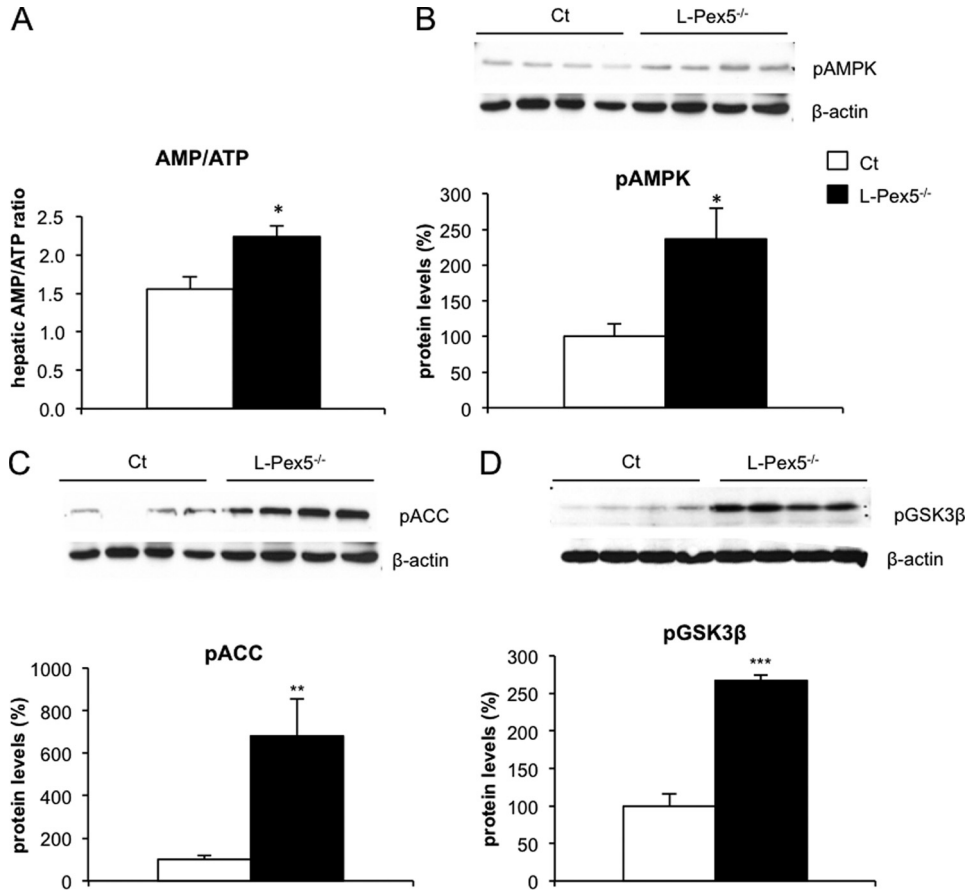

FIGURE 7. **AMPK is activated in *L-Pex5*$^{-/-}$ mice.** *A,* AMP/ATP ratio, determined by HPLC analysis, was significantly increased in *Pex5*$^{-/-}$ liver when compared with control liver. Data are shown as means ± S.E., $n = 4$. *B–D,* Western blot analysis of pAMPK (*B*, $n = 12$), pACC (*C*, $n = 8$), and pGSK3β (*D*, $n = 4$) in *L-Pex5*$^{-/-}$ mice. Levels of phosphorylated AMPK, ACC, and GSK3β were significantly higher in *L-Pex5*$^{-/-}$ mice. *L-Pex5*$^{-/-}$ *versus* control mice: ***, $p < 0.001$; **, $p < 0.01$; *, $p < 0.05$.

suppressed in livers that are deprived of functional peroxisomes.

Suppressed PGC-1α Contributes to Impaired Gluconeogenesis—PGC-1α is known to be a key regulator of hepatic gluconeogenesis. To study whether the suppressed PGC-1α activity functionally contributes to the down-regulation of gluconeogenesis in peroxisome-deficient livers, we explored whether overexpression of PGC-1α could rescue the *L-Pex5*$^{-/-}$ phenotype and therefore infected primary hepatocytes with adenovirus encoding PGC-1α. Two days after infection, we confirmed a robust increase in PGC-1α protein levels (Fig. 10*A*). Concomitantly, both *Pck1* expression and glucose secretion were induced by PGC-1α in *L-Pex5*$^{-/-}$ hepatocytes (Fig. 10, *B* and *C*). This suggests that the low PGC-1α levels and activity may contribute to the reduced gluconeogenesis in *L-Pex5*$^{-/-}$ livers. To rule out nonspecific effects, expression of genes that are not PGC-1α targets (*e.g. Slc2a2* (encoding GLUT2)) were analyzed, but their expression was not altered (Fig. 10*D*).

DISCUSSION

At first sight, peroxisomes have a secluded position in overall cellular metabolism because they handle a particular set of substrates such as very long chain fatty acids, branched chain fatty acids, and ether lipids, which are rather "rare" in cells. A notable exception is that in liver they are essential for the conversion of cholesterol into mature bile acids because of their chain shortening and conjugating activities. Peroxisomes do not directly take part in carbohydrate metabolism and energy generation from common medium and long chain fatty acids or in the synthesis of lipid storage molecules.

We previously showed that glycolytic enzyme activity is upregulated in peroxisome-deficient hepatocytes, likely to compensate for impaired oxidative phosphorylation (11), but we did not characterize glucose metabolism in detail, nor did we examine the underlying mechanisms. We now studied these metabolic changes in more detail and show that, besides an induction of glycolysis, hepatic deficiency of PEX5 also reduces gluconeogenesis, impairs repletion of glycogen stores, and causes insulin resistance. Our data thus provide new fundamental molecular insight into how liver PEX5 deficiency induces this extensive metabolic reprogramming. Therefore, peroxisome deficiency has an important indirect effect on the maintenance of carbohydrate homeostasis in the rodent liver. An overview of the observed deregulations and of potential mechanisms is given in Fig. 11.

In vivo calorimetric measurements demonstrated increased catabolism of glucose in *Pex5*$^{-/-}$ livers, which was in line with increased food intake and lower body weights. This was corrob-

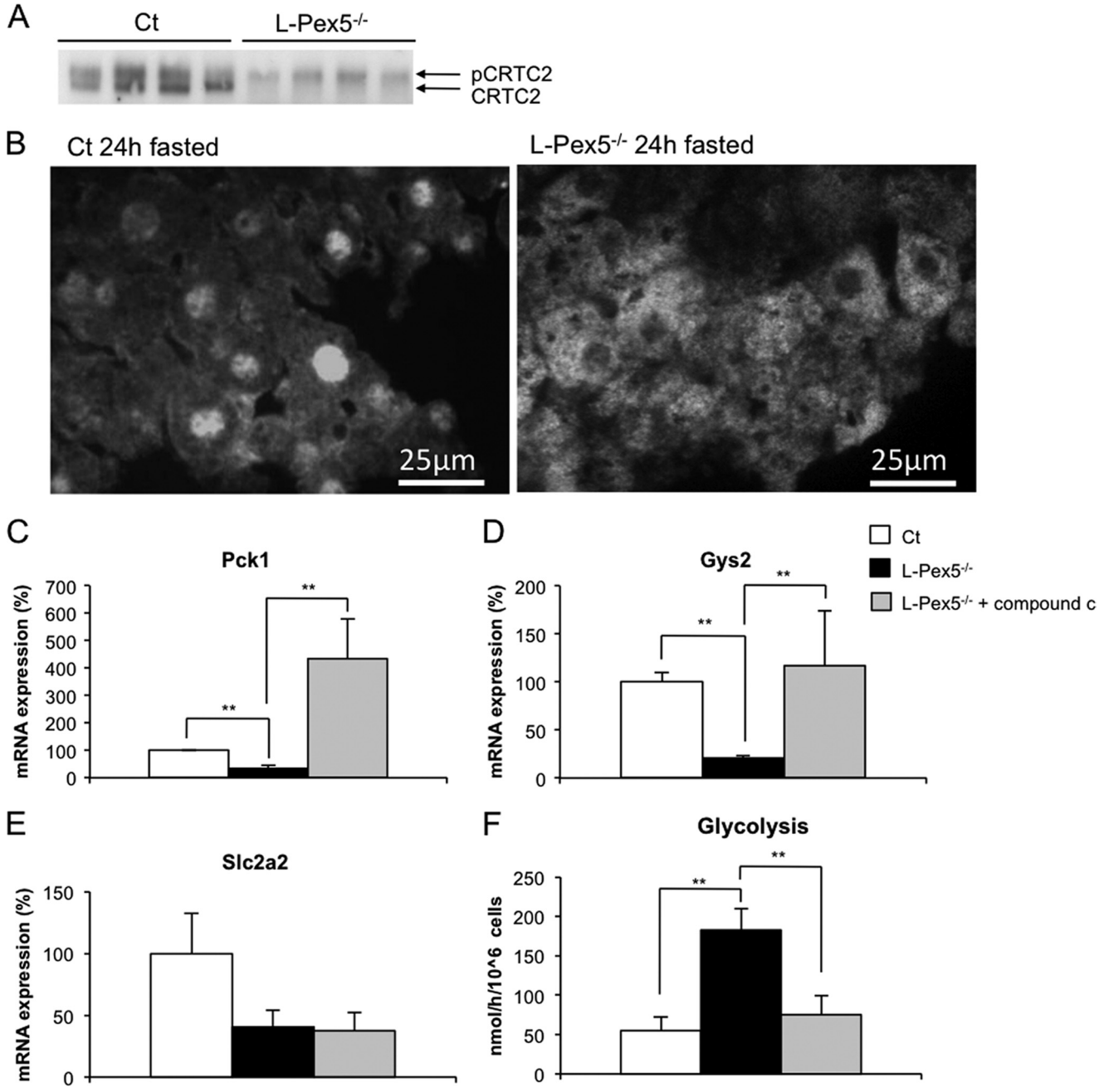

FIGURE 8. **AMPK activation contributes to deregulation of carbohydrate metabolism.** *A,* Western blot analysis of CRTC2 shows increased CRTC2 phosphorylation in *L-Pex5*$^{-/-}$ livers ($n = 4$). *B,* subcellular localization of CRTC2. Upon fasting, CRTC2 migrates to the nucleus in wild type hepatocytes, whereas CRTC2 is excluded from the nucleus in fasted *L-Pex5*$^{-/-}$ livers. Expression levels of *Pck1* (*C*), *Gys2* (*D*), and *Slc2a2* (GLUT2) (*E*) in primary hepatocytes treated with vehicle or with 10 μM compound c. Inhibition of AMPK reversed the suppression of *Pck1* and *Gys2* in *Pex5*$^{-/-}$ hepatocytes, although *Slc2a2* (GLUT2) expression levels were not influenced. Expression levels are shown relative to levels in wild type hepatocytes, which were set to 100%. *F,* glycolytic flux normalized after inhibition of AMPK by compound c (shown as nmol glucose/h/10^6 cells). All values are given as means ± S.E., $n = 4$. *Pex5*$^{-/-}$ *versus* control hepatocytes or compound c *versus* vehicle-treated *Pex5*$^{-/-}$ hepatocytes: **, $p < 0.01$.

orated by an increased glycolytic flux in cultured hepatocytes and enhanced post-glycolytic usage of pyruvate. Indeed, activity of PDH, which converts pyruvate to acetyl-CoA and links glycolysis with mitochondrial metabolism of pyruvate via the TCA cycle, was increased. This may, at first sight, appear surprising in view of the 8-fold increased mRNA expression of PDK4, one of the kinases that inhibits PDH activity. PDK4 is a well established PPARα target that is induced during fasting (47). This apparent inconsistency may, however, be explained by the finding that mRNA levels of the most abundant hepatic pyruvate dehydrogenase kinase isoform, PDK2, were not altered. In addition, the activation of PDKs also requires increased cellular levels of acetyl-CoA generated by fatty acid oxidation (48), which are not expected to be increased in livers of fed mice that mainly rely on glucose oxidation. Besides entering the TCA cycle at elevated rates, pyruvate was also metabolized to lactate at increased levels (by 80%) in livers of *L-Pex5*$^{-/-}$ mice (11). Because conversion of pyruvate to lactate

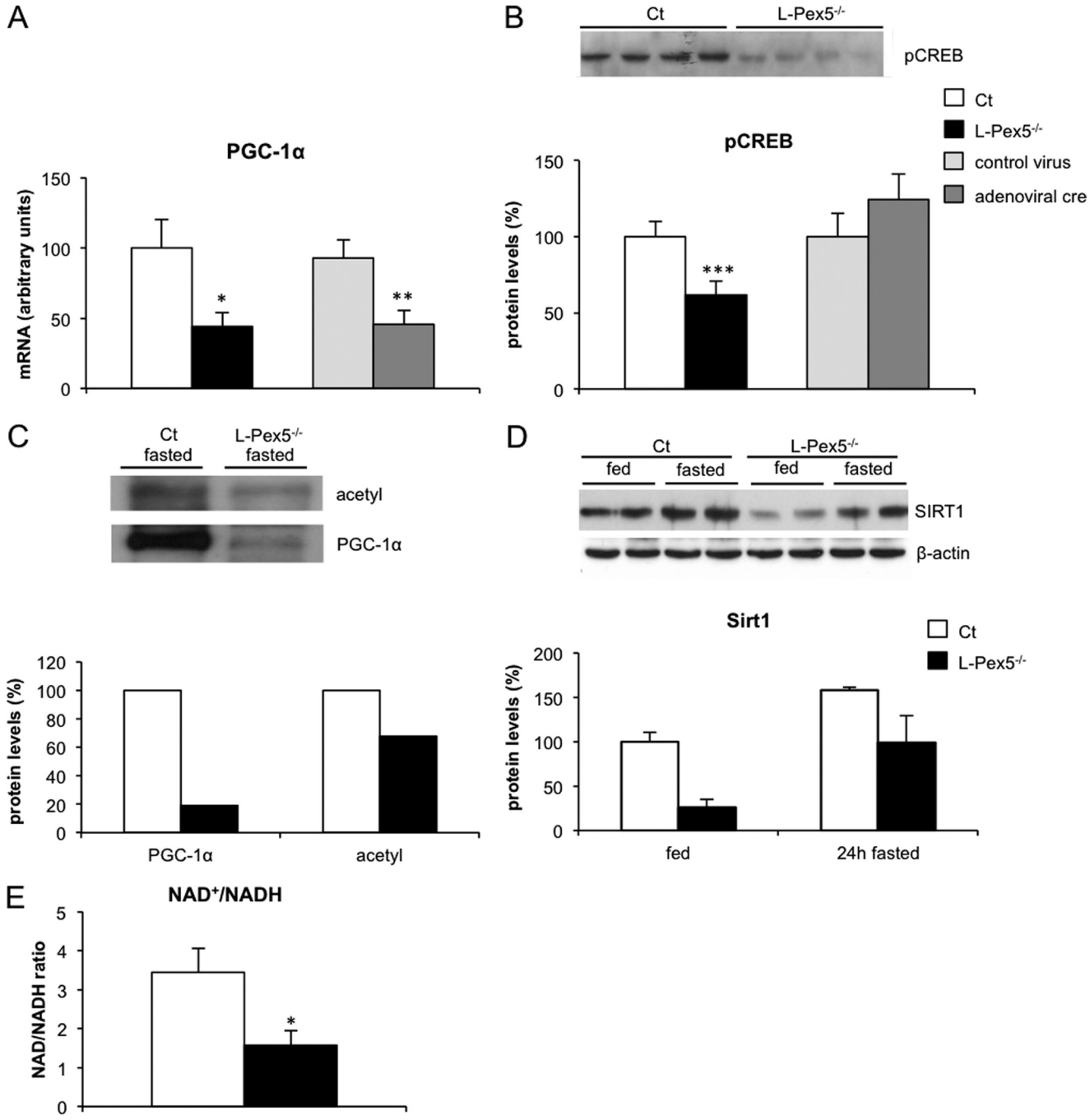

FIGURE 9. **Expression and activity of PGC-1α are suppressed in *Pex5*$^{-/-}$ liver.** *A,* hepatic transcript levels of PGC-1α were suppressed after long term (*L-Pex5*$^{-/-}$ mice) and short term (adenoviral Cre) elimination of functional peroxisomes. Expression levels were normalized to *β-actin*, and values are given as means ± S.E., $n = 4$. *B,* Western blot analysis of phosphorylated CREB shows reduced levels in livers with chronic (*L-Pex5*$^{-/-}$ mice) but not with acute (adenoviral Cre) deletion of peroxisomes ($n = 8$). A representative blot is shown. *C,* acetylation state of PGC-1α was increased in *L-Pex5*$^{-/-}$ mice. Immunoprecipitation of PGC-1α showed strongly reduced PGC-1α protein levels in *Pex5*$^{-/-}$ livers, whereas acetylation levels were similar. A representative blot and quantification is shown. *D,* Western blot analysis of SIRT1 protein levels in fasted and in fed *L-Pex5*$^{-/-}$ mice ($n = 2$). *E,* hepatic NAD$^+$/NADH ratio was significantly decreased in *L-Pex5*$^{-/-}$ mice. Data are shown as means ± S.E., $n = 4$. Knock-out *versus* respective control mice: ***, $p < 0.001$; **, $p < 0.01$; *, $p < 0.05$.

allows regeneration of NAD$^+$, a necessary cofactor for glycolysis, the glycolytic flux can be maintained at higher levels. Overall, glycolytic flux is strongly increased, providing increased amounts of pyruvate that is further metabolized via both post-glycolytic paths.

Impaired gluconeogenic capacity was evidenced by reduced transcript and/or activity levels of enzymes and transporters, by lower glycemic response to pyruvate *in vivo,* and by reduced glucose output from cultured hepatocytes. Despite this impaired ability to synthesize glucose, glycemia was normal even after fasting. Although this may seem unexpected, also *CRTC2*$^{-/-}$ mice remain normoglycemic despite impaired gluconeogenic gene transcription in liver (49). Similarly, even complete hepatic deletion of *Pck1* does not affect glycemia (50),

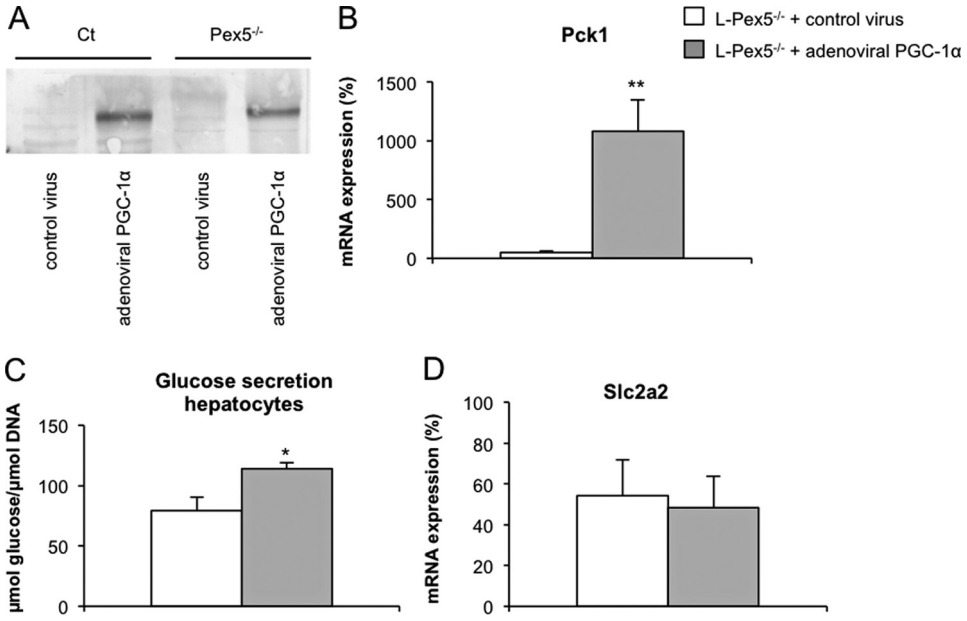

FIGURE 10. **Expression of PGC-1α in *Pex5*$^{-/-}$ hepatocytes partially reverses inhibition of gluconeogenesis.** *A,* PGC-1α protein levels were robustly increased in primary hepatocytes 2 days after infection with adenoviral PGC-1α. *B,* hepatic gene expression levels of *Pck1* were significantly induced by adenovirus-mediated expression of PGC-1α in primary *L-Pex5*$^{-/-}$ hepatocytes. *C,* expression of PGC-1α-induced glucose secretion in primary *L-Pex5*$^{-/-}$ hepatocytes ($n = 4$). *D,* hepatic gene expression levels of *Slc2a2* (GLUT2) were not affected by PGC-1α expression in *L-Pex5*$^{-/-}$ hepatocytes. Expression levels were normalized to β-*actin*, and data are shown as % of expression in control hepatocytes $\pm$ S.E., $n = 4$. PGC-1α overexpression *versus* control virus-treated hepatocytes: ***, $p < 0.001$; **, $p < 0.01$; *, $p < 0.05$.

which was explained by increased extrahepatic gluconeogenesis together with reduced glucose utilization. Interestingly, maintenance of glycemia in *L-Pex5*$^{-/-}$ mice became problematic when carbohydrate supply in the diet was limited chronically, indicating that the hepatic glucose synthesizing capacity is indeed reduced and that this deficit is functionally important.

Also the synthesis of glycogen was impaired in *L-Pex5*$^{-/-}$ hepatocytes, which was obvious by the slow restoration of glycogen stores during refeeding after a fasting period. *Gys2* transcripts were strongly suppressed in *L-Pex5*$^{-/-}$ mice, and expression of Gsk3β, a GYS2 inhibiting kinase, was concomitantly increased. Moreover, because of increased glycolytic rates in *Pex5*$^{-/-}$ livers, lower pools of glucose are expected to be available for the synthesis of glycogen.

In recent years, both glycogen synthesis and gluconeogenesis were shown to be affected by PPARα (51), but conflicting results have been reported (33). Our findings extend this ongoing debate. Indeed, because *Gys2, Pck1,* and *Slc2a2* transcripts were also reduced when peroxisomes were deleted in a *Ppar*α-deficient background, the suppression of glycogen synthesis and gluconeogenesis in *L-Pex5*$^{-/-}$ mice occurs independently of and, even more, despite the pronounced PPARα activation.

A striking observation is that hepatic PEX5 deficiency activates catabolic processes such as glycolysis and fatty acid oxidation (28, 32), while impairing anabolic processes such as glycogen synthesis and gluconeogenesis, but also *de novo* fatty acid synthesis (as already previously reported (32)). This array of metabolic adaptations is compatible with activation of AMPK, which is driven by an increased cellular AMP/ATP ratio (52). In *L-Pex5*$^{-/-}$ livers, we indeed found evidence for energy shortage, likely the consequence of structural and functional abnormalities at the inner mitochondrial membrane (11). This finding thus also implies that the high glycolytic rate is apparently not sufficient to maintain cellular AMP/ATP ratios. The resultant activation of AMPK launches an energy preservation program that in the acute phase consists of altering enzyme activities that are subsequently followed by changes at the transcriptional level, all mediated by diverse Ser/Thr phosphorylations. We found evidence for increased phosphorylation of several AMPK targets involved in diverse pathways as follows: ACC, GSK3β, and CRTC2. In addition, blocking AMPK activity with the inhibitor compound c reversed several of the metabolic anomalies in cultured *Pex5*$^{-/-}$ hepatocytes.

AMPK is well known to stimulate glycolysis, but, remarkably enough, the glycolytic target of AMPK in the liver has not been identified yet. In other cell types such as cardiomyocytes (53), monocytes, and macrophages (54), AMPK stimulates glycolysis by activating PFK2, also termed PFKFB3. This increases the synthesis of F2,6BP, which is a potent allosteric stimulator of glycolysis. However, it has been reported that AMPK does not affect the liver isoforms of PFK2 (55). In accordance with these reports, levels of F2,6BP were not elevated in *L-Pex5*$^{-/-}$ livers. Because transcript levels of rate-limiting glycolytic enzymes were not altered, it remains to be determined how glycolytic flux is elevated in peroxisome-deficient hepatocytes. One plausible contributing mechanism may be that the rate-limiting enzyme PFK1, whose activity is allosterically reduced by ATP, is released from this inhibition due to the reduced ATP levels and energy shortage in *L-Pex5*$^{-/-}$ mice. Several different mechanisms by which AMPK suppresses gluconeogenesis have been reported (41), of which some also seemed to be operational in peroxisome-deficient hepatocytes.

First, we showed that in *L-Pex5*$^{-/-}$ livers, the CREB coactivator CRTC2 was highly phosphorylated and excluded from the

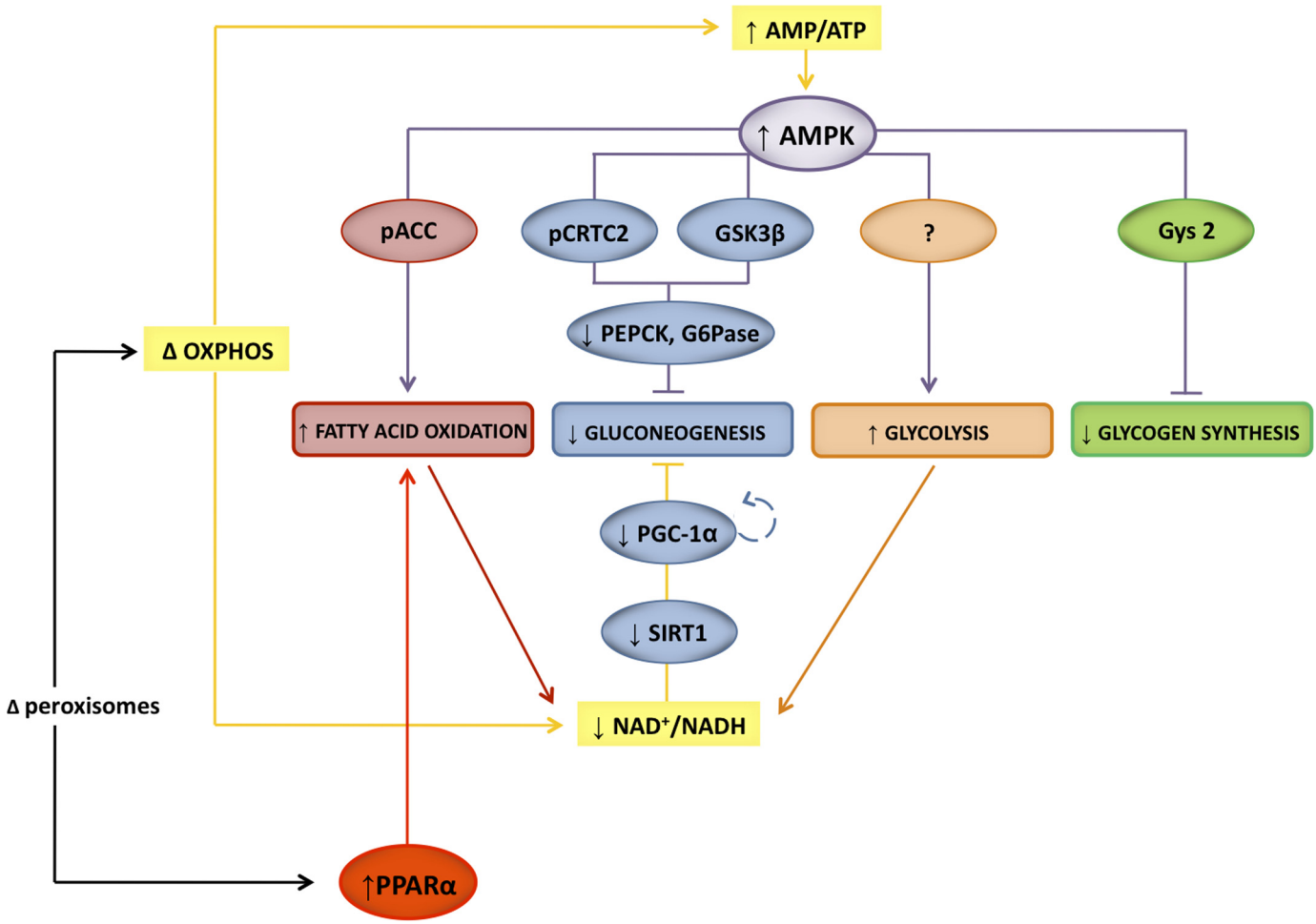

FIGURE 11. **Schematic representation of the metabolic abnormalities in *Pex5*$^{-/-}$ liver and its potential mechanisms.** Peroxisome deficiency in hepatocytes triggers, through unresolved mechanisms, a deficit in oxidative phosphorylation in mitochondria. This results in an increased AMP/ATP ratio causing AMPK activation and in a reduced NAD^+/NADH ratio, inactivating SIRT1 and PGC-1α. Simultaneously, PPARα is activated, and PGC-1α expression is down-regulated, possibly in part a result of the hampered autoregulatory feedback loop. Together, this leads to increased fatty acid β-oxidation, reduced gluconeogenesis, enhanced glycolysis, and impaired glycogen synthesis.

nucleus, which prevents transcriptional activation of gluconeogenic genes. Second, phosphorylation of GSK3β was increased, which has been reported to contribute to the suppression of PEPCK (42). Several additional mechanisms through which AMPK may suppress gluconeogenic gene expression have been reported, such as phosphorylation of FOXO1 and HNF4α, but these were not experimentally tested in our model, given the already profound effects on CRTC2 and GSK3β. Notably, inhibition of AMPK by compound c restored *Pck1* and *G-6-Pase* expression levels in *L-Pex5*$^{-/-}$ primary hepatocytes, functionally establishing the important role of AMPK in orchestrating the metabolic adaptations to loss of PEX5.

To conserve energy, activated AMPK also shuts down glycogen synthesis, as this is an anabolic energy-consuming process. We did not check for an acute effect of AMPK on GYS2 phosphorylation, which inhibits enzyme activity (57), but observed that *Gys2* transcripts were strongly suppressed in *L-Pex5*$^{-/-}$ mice. Importantly, *Gys2* expression normalized after treatment with the AMPK inhibitor compound c.

With regard to the consequences of activated AMPK on lipid metabolism, we previously documented in *L-Pex5*$^{-/-}$ mice that lipogenesis is reduced (32) and that fatty acid oxidation is stimulated *in vitro* (28) and *in vivo* (32), in agreement with increased phosphorylation of ACC. Nonetheless, despite this increased capacity for lipid catabolism, *L-Pex5*$^{-/-}$ hepatocytes are unable to maintain their energy balance.

Besides activation of AMPK, the most striking observation was the suppression of PGC-1α, another essential regulator of energy metabolism. Both transcript and protein levels of this coactivator were significantly reduced (30% of wild type levels). Importantly, PGC-1α activity is strongly determined by post-transcriptional modifications, including acetylation, phosphorylation, methylation, and ubiquitination. Of these, reversible acetylation has emerged as the most important modifier (58).

PGC-1α is deacetylated and thereby activated through SIRT1, a NAD^+-dependent deacetylase, and it is acetylated and inactivated through GCN5 (58). We demonstrated that the acetylation status of PGC-1α is increased in *L-Pex5*$^{-/-}$ livers, which indicates that not only the expression but also the activity of PGC-1α is suppressed. Furthermore, in *L-Pex5*$^{-/-}$ livers, NAD^+/NADH levels are reduced, which is probably caused by the combination of increased production of NADH through glucose and/or fatty acid oxidation and inefficient reoxidation of NADH to NAD^+ by oxidative phosphorylation (11). As a

result of the low NAD^+/NADH ratio, SIRT1 becomes less activated. Remarkably, SIRT1 protein levels were also reduced, and *Gcn5* transcripts were increased concomitantly. PGC-1α is a key driving factor of gluconeogenesis by coactivating FOXO1, HNF4α and the glucocorticoid receptor (43–46). We showed that reduced PGC-1α activity may contribute to impaired gluconeogenesis in *L-Pex5*$^{-/-}$ mice. Indeed, overexpression of the coactivator in *Pex5*$^{-/-}$ hepatocytes reversed the suppressed gluconeogenic gene expression and glucose production in *Pex5*$^{-/-}$ hepatocytes.

The relationship between AMPK and PGC-1α in the liver with regard to their opposing impact on gluconeogenesis lacks a unifying understanding. In muscle, it is well established that AMPK stimulates mitochondrial biogenesis and fatty acid oxidation by transcriptional mechanisms, orchestrated via the induction of PGC-1α (41, 59). Increased PGC-1α expression is achieved by AMPK-dependent phosphorylation of PGC-1α itself, which induces its own mRNA levels via an autoregulatory loop.

By contrast, in the liver, the situation is much more complex and unclear. When this organ experiences conditions of energy shortage, not only fatty acid oxidation needs to be turned on but, coincidently, gluconeogenesis needs to be shut down. As PGC-1α is a key driving factor of gluconeogenesis, the reported induction of PGC-1α expression and deacetylation by AMPK in the liver (41) is diametrically opposed to the role of AMPK in lowering hepatic glucose output (60–62). To reconcile these conflicting mechanisms, it has been proposed that, via phosphorylation, AMPK removes key transcription factors, which are coactivated by PGC-1α, from gluconeogenic genes, for example by inducing HNF4α instability or by redirecting FOXO to other gene promoters (41). In fact, our findings of a simultaneous activation of AMPK and suppression of PGC-1α activity in *Pex5*$^{-/-}$ livers might well be a paradigm of more general importance, which might help to resolve the debated situation in normal liver. Indeed, such opposite regulation of AMPK and PGC-1α is, for liver cells, a more "logical" mechanism to reduce gluconeogenesis.

At the same time, we appreciate that a number of other observations remain to be further clarified in the future. For instance, given that PGC-1α is an established coactivator of PPARα, how then can reduced PGC-1α levels lead to an up-regulation of PPARα target genes in *Pex5*$^{-/-}$ hepatocytes (32). Equally outstanding is the finding that PGC-1α suppression is accompanied by increased mitochondrial proliferation (11).

Apart from the fact that reduced transcript levels of PGC-1α have been seldom reported, the mechanisms through which this coactivator can be suppressed remain largely unknown. We speculate that the autoregulatory loop, whereby reduced PGC-1α activity, because of increased acetylation, further lowers PGC-1α mRNA levels might perhaps contribute to our findings. Such a mechanism was documented in SIRT1-deficient hepatocytes, in which impaired deacetylation and thus activity of PGC-1α resulted in reduced PGC-1α mRNA expression (63).

Another possibility is the increased phosphorylation of CRTC2 by AMPK, which prevents the coactivation of CREB. This should not only lower the expression of gluconeogenic genes such as PEPCK and G-6-Pase, but also the transcription of PGC-1α, which is primarily driven by the cAMP pathway. Hence, the latter mechanism might provide an explanation for our findings, although it is in contradiction with reported stimulatory effects of AMPK on PGC-1α in the normal liver (41). Additional mechanisms that possibly depend directly on the absence of functional peroxisomes can however not be excluded.

In conditions of chronic peroxisome ablation, insulin signal transduction was impaired. At first, this seemed to be explainable by the strong 41-fold induction of *Trib3*, a PPARα target, which was claimed to be an inhibitor of AKT phosphorylation and thus can cause insulin resistance (34–36). Other investigators, however, could not confirm such a role for TRIB3 in the insulin transduction pathway (37, 38). Because acute deletion of peroxisomes still up-regulated *Trib3* levels 8-fold, but did not affect insulin signaling, it seems therefore to be less likely that TRIB3 causes insulin resistance in peroxisome-deficient livers. It is worth noting that fatty liver, reduced PGC-1α, and reduced oxidative phosphorylation levels have been associated with insulin resistance and type 2 diabetes in humans and mice (45, 64, 65), although reduced PGC-1α levels have also been linked to an improvement of insulin sensitivity (66). In view of the extensive hepatosteatosis in peroxisome-deficient livers (2.2-fold increase of triglycerides (32)), the most plausible explanation may well be that this lipid accumulation causes reduced insulin signaling. In the liver, insulin resistance normally is associated with an impaired suppression of gluconeogenesis that contributes to hyperglycemia in type 2 diabetes patients. By contrast, in *L-Pex5*$^{-/-}$ livers, gluconeogenesis is reduced, despite insulin resistance, thus indicating that the mechanisms that lower gluconeogenesis must be dominant over the ones causing insulin resistance.

We conclude that peroxisome deficiency indirectly affects glucose homeostasis in hepatocytes through several different pathways. In the absence of functional peroxisomes, mitochondrial oxidative metabolism and ATP production is disturbed, causing AMPK activation that initiates an energy conservation program through enzymatic and transcriptional mechanisms. Activated AMPK shuts down gluconeogenesis and glycogen synthesis and stimulates glycolysis in an attempt to restore cellular energy balance. Concomitantly, impaired activity of PGC-1α contributes to suppression of gluconeogenesis. The precise relationship between AMPK and PGC-1α in peroxisome-deficient liver remains to be resolved. Because most metabolic disturbances seem to be caused by the shortage in mitochondrial ATP production, the peroxisome-deficient liver can be considered as a secondary mitochondrial hepatopathy (56), and it could be used as a model system for the metabolic consequences of impaired mitochondrial ATP generation in liver. Because mitochondrial abnormalities were also reported in livers of patients with a severe Zellweger syndrome phenotype, it would be interesting to examine whether they develop similar metabolic deregulations.

Acknowledgments—We thank Lies Pauwels, Benno Das, Gerd Van der Hoeven, Sabine Wyns, Sandra Jansen, Maria De Mol, and Marie-Agnès Gueuning for excellent technical help.

REFERENCES

1. Wanders, R. J., and Waterham, H. R. (2006) *Annu. Rev. Biochem.* **75,** 295–332
2. Schrader, M., and Fahimi, H. D. (2006) *Biochim. Biophys. Acta* **1763,** 1755–1766
3. Steinberg, S. J., Dodt, G., Raymond, G. V., Braverman, N. E., Moser, A. B., and Moser, H. W. (2006) *Biochim. Biophys. Acta* **1763,** 1733–1748
4. Jevon, G. P., and Dimmick, J. E. (1998) *Pediatr. Dev. Pathol.* **1,** 179–199
5. Goldfischer, S., Moore, C. L., Johnson, A. B., Spiro, A. J., Valsamis, M. P., Wisniewski, H. K., Ritch, R. H., Norton, W. T., Rapin, I., and Gartner, L. M. (1973) *Science* **182,** 62–64
6. Trijbels, J. M., Berden, J. A., Monnens, L. A., Willems, J. L., Janssen, A. J., Schutgens, R. B., and van den Broek-Van Essen, M. (1983) *Pediatr. Res.* **17,** 514–517
7. Pfeifer, U., and Sandhage, K. (1979) *Virchows Arch. A Pathol. Anat. Histol.* **384,** 269–284
8. Mooi, W. J., Dingemans, K. P., van den Bergh Weerman, M. A., Jöbsis, A. C., Heymans, H. S., and Barth, P. G. (1983) *Ultrastruct. Pathol.* **5,** 135–144
9. Mathis, R. K., Watkins, J. B., Szczepanik-Van Leeuwen, P., and Lott, I. T. (1980) *Gastroenterology* **79,** 1311–1317
10. Hughes, J. L., Poulos, A., Robertson, E., Chow, C. W., Sheffield, L. J., Christodoulou, J., and Carter, R. F. (1990) *Virchows Arch. A Pathol. Anat. Histopathol.* **416,** 255–264
11. Dirkx, R., Vanhorebeek, I., Martens, K., Schad, A., Grabenbauer, M., Fahimi, D., Declercq, P., Van Veldhoven, P. P., and Baes, M. (2005) *Hepatology* **41,** 868–878
12. Baes, M., Dewerchin, M., Janssen, A., Collen, D., and Carmeliet, P. (2002) *Genesis* **32,** 177–178
13. Postic, C., Shiota, M., Niswender, K. D., Jetton, T. L., Chen, Y., Moates, J. M., Shelton, K. D., Lindner, J., Cherrington, A. D., and Magnuson, M. A. (1999) *J. Biol. Chem.* **274,** 305–315
14. Lee, S. S., Pineau, T., Drago, J., Lee, E. J., Owens, J. W., Kroetz, D. L., Fernandez-Salguero, P. M., Westphal, H., and Gonzalez, F. J. (1995) *Mol. Cell. Biol.* **15,** 3012–3022
15. van den Berg, S. A., Nabben, M., Bijland, S., Voshol, P. J., van Klinken, J. B., Havekes, L. M., Romijn, J. A., Hoeks, J., Hesselink, M. K., Schrauwen, P., and van Dijk, K. W. (2010) *Metabolism* **59,** 1612–1618
16. Péronnet, F., and Massicotte, D. (1991) *Can. J. Sport Sci.* **16,** 23–29
17. Baes, M., Huyghe, S., Carmeliet, P., Declercq, P. E., Collen, D., Mannaerts, G. P., and Van Veldhoven, P. P. (2000) *J. Biol. Chem.* **275,** 16329–16336
18. Rodgers, J. T., Lerin, C., Haas, W., Gygi, S. P., Spiegelman, B. M., and Puigserver, P. (2005) *Nature* **434,** 113–118
19. Katoh, Y., Takemori, H., Lin, X. Z., Tamura, M., Muraoka, M., Satoh, T., Tsuchiya, Y., Min, L., Doi, J., Miyauchi, A., Witters, L. A., Nakamura, H., and Okamoto, M. (2006) *FEBS J.* **273,** 2730–2748
20. Uebi, T., Tamura, M., Horike, N., Hashimoto, Y. K., and Takemori, H. (2010) *Am. J. Physiol. Endocrinol. Metab* **299,** E413–E425
21. Jomain-Baum, M., and Schramm, V. L. (1978) *J. Biol. Chem.* **253,** 3648–3659
22. Rajas, F., Croset, M., Zitoun, C., Montano, S., and Mithieux, G. (2000) *Diabetes* **49,** 1165–1168
23. Van Veldhoven, P. P., Baumgart, E., and Mannaerts, G. P. (1996) *Anal. Biochem.* **237,** 17–23
24. Keppler, D., and Decker, K. (1984) in *Methods of Enzymatic Analysis. Metabolites 1: Carbohydrates* (Bergmeyer, H. U., ed) pp. 11–18, Verlag Chemie, Weinheim, Germany
25. Van Veldhoven, P., Declercq, P. E., Debeer, L. J., and Mannaerts, G. P. (1984) *Biochem. Pharmacol.* **33,** 1153–1155
26. Manfredi, G., Yang, L., Gajewski, C. D., and Mattiazzi, M. (2002) *Methods* **26,** 317–326
27. Van Schaftingen, E., Lederer, B., Bartrons, R., and Hers, H. G. (1982) *Eur. J. Biochem.* **129,** 191–195
28. Dirkx, R., Meyhi, E., Asselberghs, S., Reddy, J., Baes, M., and Van Veldhoven, P. P. (2007) *Biochem. Biophys. Res. Commun.* **357,** 718–723
29. Lerin, C., Rodgers, J. T., Kalume, D. E., Kim, S. H., Pandey, A., and Puigserver, P. (2006) *Cell Metab.* **3,** 429–438
30. Aragonés, J., Schneider, M., Van Geyte, K., Fraisl, P., Dresselaers, T., Mazzone, M., Dirkx, R., Zacchigna, S., Lemieux, H., Jeoung, N. H., Lambrechts, D., Bishop, T., Lafuste, P., Diez-Juan, A., Harten, S. K., Van Noten, P., De, Bock, K., Willam, C., Tjwa, M., Grosfeld, A., Navet, R., Moons, L., Vandendriessche, T., Deroose, C., Wijeyekoon, B., Nuyts, J., Jordan, B., Silasi-Mansat, R., Lupu, F., Dewerchin, M., Pugh, C., Salmon, P., Mortelmans, L., Gallez, B., Gorus, F., Buyse, J., Sluse, F., Harris, R. A., Gnaiger, E., Hespel, P., Van Hecke, P., Schuit, F., Van Veldhoven, P., Ratcliffe, P., Baes, M., Maxwell, P., and Carmeliet, P. (2008) *Nat. Genet.* **40,** 170–180
31. Martens, K., Ver Loren van Themaat, E., van Batenburg, M. F., Heinäniemi, M., Huyghe, S., Van Hummelen, P., Carlberg, C., Van Veldhoven, P. P., Van Kampen, A., and Baes, M. (2008) *Biochim. Biophys. Acta* **1781,** 694–702
32. Peeters, A., Swinnen, J. V., Van Veldhoven, P. P., and Baes, M. (2011) *Biochimie* **93,** 1828–1838
33. Peeters, A., and Baes, M. (2010) *PPAR Res.* **2010,** ii, 572405
34. Du, K., Herzig, S., Kulkarni, R. N., and Montminy, M. (2003) *Science* **300,** 1574–1577
35. Koo, S. H., Satoh, H., Herzig, S., Lee, C. H., Hedrick, S., Kulkarni, R., Evans, R. M., Olefsky, J., and Montminy, M. (2004) *Nat. Med.* **10,** 530–534
36. Wang, Y. G., Shi, M., Wang, T., Shi, T., Wei, J., Wang, N., and Chen, X. M. (2009) *World J. Gastroenterol.* **15,** 2329–2335
37. Okamoto, H., Latres, E., Liu, R., Thabet, K., Murphy, A., Valenzeula, D., Yancopoulos, G. D., Stitt, T. N., Glass, D. J., and Sleeman, M. W. (2007) *Diabetes* **56,** 1350–1356
38. Iynedjian, P. B. (2005) *Biochem. J.* **386,** 113–118
39. Koo, S. H., Flechner, L., Qi, L., Zhang, X., Screaton, R. A., Jeffries, S., Hedrick, S., Xu, W., Boussouar, F., Brindle, P., Takemori, H., and Montminy, M. (2005) *Nature* **437,** 1109–1111
40. Viollet, B., Guigas, B., Leclerc, J., Hebrard, S., Lantier, L., Mounier, R., Andreelli, F., and Foretz, M. (2009) *Acta Physiol.* **196,** 81–98
41. Cantó, C., and Auwerx, J. (2010) *Cell. Mol. Life Sci.* **67,** 3407–3423
42. Horike, N., Sakoda, H., Kushiyama, A., Ono, H., Fujishiro, M., Kamata, H., Nishiyama, K., Uchijima, Y., Kurihara, Y., Kurihara, H., and Asano, T. (2008) *J. Biol. Chem.* **283,** 33902–33910
43. Yoon, J. C., Puigserver, P., Chen, G., Donovan, J., Wu, Z., Rhee, J., Adelmant, G., Stafford, J., Kahn, C. R., Granner, D. K., Newgard, C. B., and Spiegelman, B. M. (2001) *Nature* **413,** 131–138
44. Puigserver, P., Rhee, J., Donovan, J., Walkey, C. J., Yoon, J. C., Oriente, F., Kitamura, Y., Altomonte, J., Dong, H., Accili, D., and Spiegelman, B. M. (2003) *Nature* **423,** 550–555
45. Handschin, C., and Spiegelman, B. M. (2006) *Endocr. Rev.* **27,** 728–735
46. Rhee, J., Ge, H., Yang, W., Fan, M., Handschin, C., Cooper, M., Lin, J., Li, C., and Spiegelman, B. M. (2006) *J. Biol. Chem.* **281,** 14683–14690
47. Wu, P., Peters, J. M., and Harris, R. A. (2001) *Biochem. Biophys. Res. Commun.* **287,** 391–396
48. Roche, T. E., Baker, J. C., Yan, X., Hiromasa, Y., Gong, X., Peng, T., Dong, J., Turkan, A., and Kasten, S. A. (2001) *Prog. Nucleic Acid Res. Mol. Biol.* **70,** 33–75
49. Le Lay, J., Tuteja, G., White, P., Dhir, R., Ahima, R., and Kaestner, K. H. (2009) *Cell Metab.* **10,** 55–62
50. She, P., Burgess, S. C., Shiota, M., Flakoll, P., Donahue, E. P., Malloy, C. R., Sherry, A. D., and Magnuson, M. A. (2003) *Diabetes* **52,** 1649–1654
51. Mandard, S., Stienstra, R., Escher, P., Tan, N. S., Kim, I., Gonzalez, F. J., Wahli, W., Desvergne, B., Müller, M., and Kersten, S. (2007) *Cell. Mol. Life Sci.* **64,** 1145–1157
52. Hardie, D. G., Hawley, S. A., and Scott, J. W. (2006) *J. Physiol.* **574,** 7–15
53. Marsin, A. S., Bertrand, L., Rider, M. H., Deprez, J., Beauloye, C., Vincent, M. F., Van den Berghe, G., Carling, D., and Hue, L. (2000) *Curr. Biol.* **10,** 1247–1255
54. Marsin, A. S., Bouzin, C., Bertrand, L., and Hue, L. (2002) *J. Biol. Chem.* **277,** 30778–30783
55. Hardie, D. G. (2011) *Am. J. Clin. Nutr.* **93,** 891S-6
56. Lee, W. S., and Sokol, R. J. (2007) *Hepatology* **45,** 1555–1565
57. Carling, D., and Hardie, D. G. (1989) *Biochim. Biophys. Acta* **1012,** 81–86
58. Jeninga, E. H., Schoonjans, K., and Auwerx, J. (2010) *Oncogene* **29,** 4617–4624

59. Cantó, C., Gerhart-Hines, Z., Feige, J. N., Lagouge, M., Noriega, L., Milne, J. C., Elliott, P. J., Puigserver, P., and Auwerx, J. (2009) *Nature* **458,** 1056–1060
60. Lochhead, P. A., Salt, I. P., Walker, K. S., Hardie, D. G., and Sutherland, C. (2000) *Diabetes* **49,** 896–903
61. Foretz, M., Ancellin, N., Andreelli, F., Saintillan, Y., Grondin, P., Kahn, A., Thorens, B., Vaulont, S., and Viollet, B. (2005) *Diabetes* **54,** 1331–1339
62. Viana, A. Y., Sakoda, H., Anai, M., Fujishiro, M., Ono, H., Kushiyama, A., Fukushima, Y., Sato, Y., Oshida, Y., Uchijima, Y., Kurihara, H., and Asano, T. (2006) *Diabetes Res. Clin. Pract.* **73,** 135–142
63. Purushotham, A., Schug, T. T., Xu, Q., Surapureddi, S., Guo, X., and Li, X. (2009) *Cell Metab.* **9,** 327–338
64. Patti, M. E., Butte, A. J., Crunkhorn, S., Cusi, K., Berria, R., Kashyap, S., Miyazaki, Y., Kohane, I., Costello, M., Saccone, R., Landaker, E. J., Goldfine, A. B., Mun, E., DeFronzo, R., Finlayson, J., Kahn, C. R., and Mandarino, L. J. (2003) *Proc. Natl. Acad. Sci. U.S.A.* **100,** 8466–8471
65. Mootha, V. K., Lindgren, C. M., Eriksson, K. F., Subramanian, A., Sihag, S., Lehar, J., Puigserver, P., Carlsson, E., Ridderstråle, M., Laurila, E., Houstis, N., Daly, M. J., Patterson, N., Mesirov, J. P., Golub, T. R., Tamayo, P., Spiegelman, B., Lander, E. S., Hirschhorn, J. N., Altshuler, D., and Groop, L. C. (2003) *Nat. Genet.* **34,** 267–273
66. Kumashiro, N., Tamura, Y., Uchida, T., Ogihara, T., Fujitani, Y., Hirose, T., Mochizuki, H., Kawamori, R., and Watada, H. (2008) *Diabetes* **57,** 2083–2091